Karwad, Mustafa A. and Macpherson, Tara and Wang, Bo and Theophilidou, Elena and Sarmad, Sarir and Barrett, David A. and Larvin, Michael and Wright, Karen L. and Lund, Jonathan N. and O'Sullivan, Saoirse (2016) Oleoylethanolamine and palmitoylethanolamine modulate intestinal permeability in vitro via TRPV1 and PPARα. FASEB Journal, 31 (2). pp. 469-481. ISSN 1530-6860

Oleoylethanolamine and palmitoylethanolamine modulate intestinal permeability *in vitro* via TRPV1 and PPARα: a new potential class of therapeutic agents for intestinal inflammation and hyperpermeability?

Short title: OEA and PEA modulate intestinal permeability

Mustafa A. Karwad[1], Tara Macpherson[2], Bo Wang[2], Elena Theophilidou[1], Sarir Sarmad[3], David A. Barrett[3], Michael Larvin[4], Karen L. Wright[2], Jonathan N. Lund[1] and Saoirse E. O'Sullivan[1*]

[1]School of Medicine, Royal Derby Hospital, University of Nottingham (MAK, JL, SOS)
[2]Division of Biomedical and Life Sciences, Faculty of Health and Medicine, Lancaster University (TM, BW, KLW)
[3]Centre for Analytical Bioscience, School of Pharmacy, University of Nottingham, Nottingham, NG7 2RD (SS and DAB)
[4]Graduate Entry Medical School and the Health Research Institute, University of Limerick, Limerick, Ireland (ML)

***Correspondence**

Saoirse E. O'Sullivan, School of Medicine, Royal Derby Hospital, University of Nottingham, Derby. DE22 3DT UK, E-mail: Saoirse.osullivan@nottingham.ac.uk, Phone: 01332724701

No disclosures.

Author contribution:
Conception and design of the study; David A. Barrett, Karen L. Wright, Michael Larvin, Jonathan N. Lund, Saoirse E. O'Sullivan
Generation, collection, assembly, analysis and/or interpretation of data; Mustafa A. Karwad, Tara Macpherson, Bo Wang, Elena Theophilidou, Sarir Sarmad, Karen L. Wright, Saoirse E. O'Sullivan
Drafting or revision of the manuscript; all
Approval of the final version of the manuscript: all

ABBREVIATIONS: AEA, arachidonyl ethanolamide or anandamide; Caco-2, carcinoma colon cell line; CB_1, cannabinoid receptor one; CB_2, cannabinoid receptor two; OEA, oleoylethanolamine; PEA, palmitoylethanolamine; TRPV1, transient receptor potential vanilloid subtype 1; PPAR, peroxisome proliferator-activated receptor; TEER, transepithelial electrical resistance; AM251, *N*-(piperidin-1-yl)-5-(4-iodophenyl)-1-(2,4-dichlorophenyl)- 4-methyl-1*H*-pyrazole-3-carboxamide; AM630, 6-iodo-2-methyl-1-[2-(4-morpholinyl)ethyl] -1H-indol-3-y l](4-methoxyphenyl) methanone; GW9662, 2-chloro-5-nitro-*N*-phenylbenzamide; GW6471, [(2*S*)-2-[[(1*Z*)-1-methyl-3-oxo-3-[4-(trifluoromethyl)phenyl]-1-propenyl]amino]-3-[4-[2-(5-methyl-2-phenyl-4-xazolyl)ethoxy] phenyl]propyl]-carbamic acid ethyl ester; O-1918, 1,3-dimethoxy- 5-methyl-2- (1*R*,6*R*)-3-methyl-6-(1-methylethenyl)-2-cyclohexen-1-yl]benzene; ANOVA, analysis of variance; EVOM, Epithelial tissue volt-ohm-meter; URB597, 3'-(aminocarbonyl)[1,1'-biphenyl]-3-yl)-cyclohexylcarbamate; GI, Gastro-intestinal; GPRs, G protein-coupled receptors; IFNγ, interferon-γ; TNFα, tumour necrosis factor-α; IBD, inflammatory bowel disease; FAAH, fatty acid amide hydrolase; URB597, 3'-(aminocarbonyl)[1,1'-biphenyl]-3-yl)-cyclohexylcarbamate.

Abstract

Purpose: Cannabinoids modulate intestinal permeability through CB_1. The endocannabinoid-like compounds oleoylethanolamine (OEA) and palmitoylethanolamine (PEA) play an important role in digestive regulation, and we hypothesised they would also modulate intestinal permeability.

Procedures: Trans-epithelial electrical resistance (TEER) was measured in human Caco-2 cells to assess permeability after OEA and PEA application and relevant antagonists. Cells treated with OEA and PEA were stained for cytoskeletal F-actin changes and lysed for immunoassays. OEA and PEA were measured by liquid chromatography tandem mass spectrometry.

Findings: OEA (applied apically, $LogEC_{50}$ -5.4) and PEA (basolaterally, $LogEC_{50}$ -4.9; apically $LogEC_{50}$ -5.3) increased Caco-2 resistance by 20-30% via transient receptor potential vanilloid 1 (TRPV1) and peroxisome proliferator-activated receptor alpha (PPARα). Preventing their degradation (by inhibiting fatty acid amide hydrolase), enhanced the effects of OEA and PEA. OEA and PEA induced cytoskeletal changes and activated focal adhesion kinase (FAK), extracellular signal-regulated kinases 1/2 (Erk1/2), and decreased Src kinases, and decreased aquaporins 3 and 4. In Caco-2 cells treated with IFNγ and TNFα, OEA (via TRPV1) and PEA (via PPARα) prevented or reversed the cytokine-induced increased permeability compared to vehicle (0.1% ethanol). PEA (basolateral) also reversed increased permeability when added 48h or 72h after cytokines ($P<0.001$, via PPARα). Cellular and secreted levels of OEA and PEA ($P<0.001$-0.001) were increased in response to inflammatory mediators.

Conclusion: OEA and PEA have endogenous roles and potential therapeutic applications in conditions of intestinal hyperpermeability and inflammation.

Introduction

The human gastrointestinal tract forms the largest interface between the external environment and internal milieu (1). Aside from its digestive functions, it also constitutes the most complex and most evolved element of immune defence. Intestinal epithelial cells, together with their mucous coatings, constitute a protective barrier across which paracellular permeation is selectively regulated by transmembrane protein contractility within the intercellular tight junctions (2, 3). This prevents the loss of water and solutes from the gut, whilst simultaneously permitting the absorption of water and nutrients, but preventing the ingress of toxins, antigens and pathogens (4-6). Impaired intestinal barrier function leading to hyperpermeability is associated with a wide variety of human diseases and conditions, for example acutely in shock and multiple organ-system dysfunction with splanchnic ischaemia (3), sepsis (2), or more gradually, including inflammatory bowel disease (7-10), coeliac disease (11), irritable bowel syndrome (12, 13) and a range of other conditions (14, 15). Family studies have demonstrated that increased intestinal permeability can precede the clinical presentation of inflammatory bowel disease (16-18). The regulation of intestinal permeability is poorly understood, and improved understanding is required for the development of therapeutic interventions specifically targeted at restoring normal permeability (19).

Cannabis sativa plant extracts have been used anecdotally over 5 millennia for the treatment of gastrointestinal disorders including nausea, vomiting, anorexia, intestinal inflammation and diarrhoea (20). Endocannabinoids are intercellular lipid signalling molecules derived from arachidonic acid and synthesized on demand from cell membrane precursors. Examples were found to be expressed in the gut only 20 years ago (21), and subsequently endocannabinoids and their receptors were shown to be key regulators of a variety of gastrointestinal functions including emesis (22), intestinal motility (23) and secretion (24). Endocannabinoids play significant roles in inflammation and apoptosis (25, 26) and specifically in intestinal inflammation (27), opening up the possibility of new therapeutic options (28).

Endocannabinoids exert their effects by activation of cannabinoid receptors (CB_1 and CB_2) (29) and other target sites of action such as transient receptor potential ion channels (TRPs)

(30), peroxisome proliferator-activated receptors (PPARs), (31) and orphan G-protein coupled receptors GPR119 (32) and GPR55 (33). All of these target sites are expressed in the gastrointestinal tract. These receptors, together with endocannabinoid ligands and the enzymes responsible for their metabolism, are collectively referred to as the 'endocannabinoid system' (ECS). The ECS is involved in modulating gastrointestinal motility and intestinal inflammation, and is up-regulated in intestinal inflammation. Our group has previously reported that cannabinoids modulate intestinal permeability *in vitro* using Caco-2 intestinal cells (34, 35), which has also been shown *in vivo* (36). The plant-derived cannabinoids, Δ^9tetrahydrocannabinol (THC) and cannabidiol (CBD) reversed the increased permeability caused by EDTA or cytokines via CB_1 receptor activation (34, 35). By contrast, the endocannabinoids anandamide (AEA) and 2-arachidonoylglycerol (2-AG) increased permeability of the Caco-2 monolayer via the CB_1 receptor (34, 35), and inhibiting their synthesis improved the effects of inflammation on permeability, suggesting that the endogenous production of these compounds in response to inflammation plays a role in promoting permeability changes at the epithelium.

Oleoylethanolamine (OEA) is an endocannabinoid-like compound that does not bind to cannabinoid receptors (37). OEA is produced on demand in enterocytes, and its production is stimulated by food intake (38) or reduced by food deprivation (39). OEA is a PPARα agonist (40), activates TRPV1 channels (41), and the orphan G-protein-coupled receptors GPR55 and GPR119 (42). OEA administration suppresses food intake, decreases body weight gain (43) and induces satiety via PPARα activation (44). It also has a role in lipid metabolism regulation (45), reducing cholesterol levels in mice via PPARα (40, 46). Palmitoylethanolamine (PEA) is another endocannabinoid-like compound found in high levels in the upper GI tract compared to other organs and tissues (39). PEA reduces intestinal injury and inflammation in mice via PPARα (47, 48). More recently, oral or intra-peritoneal administration of PEA was found to reduce inflammation and damage in dinitrobenzene sulfonic acid (DNBS)-induced colitis in mice, mediated by PPARα, CB_2 and GPR55 (49) and inhibition of the enzyme responsible for PEA degradation also reduces inflammation in two mouse models of colitis (50).

In the present study, we hypothesised that OEA and PEA, which often have opposing physiological actions and different pharmacology to AEA and 2-AG, might also modulate

intestinal permeability and play a role in intestinal inflammation. Specifically, we hypothesised that these compounds would have a beneficial effect on intestinal permeability based on their positive effects *in vivo* in simulated inflammation.

Materials and Methods

Cell culture

Caco-2 cells (European Collection of Cell Culture, Wiltshire, UK; passages 62-86) were cultured in T75 cell culture flask in Minimal Essential Medium Eagle supplemented with 10% fetal bovine serum, 1% penicillin/streptomycin and L-glutamine at 37°C in 5% CO2 and 95% air.

Effects of OEA and PEA on Caco-2 monolayer permeability

The cells were seeded at 20,000 cells on 6.4mm diameter, 0.4µm pore size polyethylene terephthalate inserts (BD Falcon Biosciences, UK) and grown for 14-18 days. Transepithelial electrical resistance (TEER) was measured using a voltohm meter (EVOM^2) (World Precision Instruments, Sarasota FL, USA) as an indicator of cellular permeability. Caco-2 cell monolayers with TEER value greater than 1000 $\Omega.cm^2$ were used. Caco-2 cell monolayers were washed twice in HBSS (+ N-2-hydroxyethylpintestinal permeabilityerazine-N'-2-ethanesulfonic acid or HEPES and P/S) and baseline TEER measured. Increasing concentrations of OEA or PEA (1nM to 10µM) or vehicle (0.1% ethanol) were applied in pre-warmed MEME medium to the apical or basolateral compartment of inserts, and TEER was measured over the next 48h.

The following target sites of action were investigated (receptor antagonist and concentrations shown in brackets); CB_1 (AM251, 100nM (K_i 7.49 nM)), CB_2 (AM630, 100nM (K_i 31.2 nM)), PPARγ (GW9662, 100nM (IC_{50} 3.3 nM)), PPARα (GW6471, 100nM (IC_{50} 240 nM)), TRPV1 (Capsazepine, 1µM (K_i 3.2 µM)) and proposed endothelial cannabinoid receptor antagonist (O-1918, 1µM). In some experiments, OEA and PEA (3µM) were applied with an inhibitor of their degradation by fatty acid amide hydrolase (FAAH), using URB597 (1µM), in absence and presence of capsazepine or GW6471.

To simulate inflammatory conditions, 10ng.ml^{-1} of Interferon-γ (IFNγ) was added basolaterally. After 8h, 10ng.ml^{-1} tumour necrosis factor-α (TNFα) was added for another 16

h. OEA and PEA were added to the apical or basolateral compartment at various time points, either at the same time as IFNγ (time 0h, to potentially block the development of inflammation), or after the induction of inflammation (at 24h, 48h or 72 h) to potentially limit the inflammatory increase in permeability). In some experiments, this was done in the presence of antagonists. For prolonged (chronic) inflammatory studies (see Figure 6), repeated applications of 3 $ng.ml^{-1}$ of INFγ and TNFα were used.

Cell viability assays

To test the effects of OEA and PEA on cell viability in fully differentiated Caco-2 cells, Cells were brought to confluence and maintained in complete medium for up to 18 days in 96-well plates. A concentration response to OEA and PEA was then performed in complete medium over 48 hours, after which PrestoBlue™ Reagent (Life Technologies, Paisley, UK) was added directly to the cell culture (1:10). After 10 minutes, absorbance was measured with excitation at 570 nm with 600 nm as reference wavelength for normalization. Data was calculated as the mean per cent change from untreated control.

To test the effects of OEA and PEA on cell viability in proliferating Caco-2 cells, 5x10^3 cells were seeded in quadruplicate into a 96-well microplate in standard medium with 8% serum. A series dilution of OEA and PEA from 10 μM was performed across the plate. Cells were incubated for 72 hours. Growth medium was carefully removed and 50μl of 1x CyQUANT® NF dye reagent (Life technologies) was added to each well. The microplate was incubated at 37°C for 30 minutes and fluorescence intensity of each sample was measured using a fluorescence microplate reader (Tecan) with excitation at ~485 nm and emission detection at ~530 nm. Data was calculated as the mean of the % untreated control.

Phalloidin staining

Phalloidin is an F-actin stain that allows for the visualisation of the structure and inferred function of this cytoskeletal filament protein. Cells are fixed first so the image is a snapshot of the given timepoint. Linear actin fibres (mostly parallel) are the polymerised F-actin in the cytoplasm and can be quite pronounced at the cell boundaries or at focal adhesion plaques. Changes in the network can be a result of disruption or required changes for movement and changes to adhesion. For this experiment, cells were grown on 8 well chamber slides (BD Bioscience, Oxford, UK) for 16-18 days and fixed in 4% paraformaldehyde for 45 min at RT after the indicated treatments. Cells were then washed in PBS before permeabilisation with

0.5%Triton™X-100. Cells were blocked in 5% bovine serum albumin in PBS for 20 min at RT and incubated with phalloidin tetramethylrhodamine B isothiocyanate (TRITC)-conjugated solution 5 Units/ml (a kind donation from Dr Alan Shirras, Faculty of Health and Medicine, Lancaster University, UK) for 20 min at RT. Cells were washed 3 times with PBS and mounted with VECTASHIELD®Mounting Media containing 4',6-diamidino-2-phenylindole (DAPI, VECTOR LABORATORIES Ltd. Peterborough, UK). Stained cells were viewed on a Zeiss Confocal microscope at ×63 magnification.

Immunoassays

For all immunoassay experiments, Caco-2 ells were grown in 6 or 12 well culture plates and treated with OEA and PEA at the apical membrane. After treatment protocols, the cells were washed in PBS and lysed in RIPA buffer (150 mM NaCl, 1.0% IGEPAL® CA-630, 0.5% sodium deoxycholate, 0.1% SDS, and 50 mM Tris, pH 8.0) with protease inhibitor cocktail (#P8340, Sigma, UK). Protein content of lysates was determined using Bradford reagent.

For western blotting, fifteen micrograms (15 μg) of protein was then processed on a precast 10% SDS-PAGE gel and transferred onto nitrocellulose membrane (BioRad, Hertfordshire, UK) before blocking with Protein-free Tris-buffered saline (TBS) blocking buffer (#10269613, Thermo Scientific Pierce, Rockford, USA) in with 0.1% Tween (TBST) at RT for 1 h. Primary antibodies (Cell Signaling, New England Biolabs, Hertfordshire, UK) were incubated overnight at 4°C as follows: Phospho-FAK (Tyr397) (D20B1) Rabbit mAb (#8556P, 1:1000), Phospho-p44/42 MAPK (Erk1/2) (Thr202/Tyr204) (E10) Mouse mAb (#9106, 1:1000) and anti- β-Actin (D6A8) Rabbit mAb (#8457, 1:1000). After washing extensively with TBS plus 0.1% Tween (TBST), secondary anti-mouse or anti-rabbit IgG, HRP-linked antibodies, at 1:10,000 (Cell Signaling, New England Biolabs, Hertfordshire, UK) were applied to membranes at room temperature for 1 h. Blots were exposed using Clarity™ Western ECL Substrate (BioRad, Hertfordshire, UK) and imaged with the BioRad ChemiDoc™ XRS system. These experiments were performed on four separate occasions.

To further elucidate the potential signalling proteins involved, Luminex® xMAP® technology was used to detect changes in phosphorylated CREB (pS133), ERK (pT185/pY187), NFκB (pS536), JNK (pT183/pY185), p38 (pT180/pY182), p70 S6K (pT412), STAT3 (pS727), STAT5A/B (pY694/699) and Akt (pS473) (Milliplex™, 48-680MAG, Merck Millipore) and Blk (Tyr389), Fgr (Tyr412), Fyn (Tyr420), Hck (Tyr411), Lck (Tyr394), Lyn (Tyr397), Src (Tyr419) and Yes (Tyr421)(Milliplex™, 48-650MAG

Human Src Family kinase, Merck Millipore) in cell lysates lysed with RIPA buffer and protease and phosphatase inhibitors.

To detect changes in aquaporin expression at the cell membrane, the Mem-Per™ Plus Membrane protein extraction kit was used to isolate the membrane protein fraction, and commercially available ELISAs were used to measure aquaporin 3 (LS-F13078, LifeSpan Biosciences Inc) and aquaporin 4 (LS-F13079, LifeSpan Biosciences Inc.)

Potassium channel activation

To test the ability of OEA and PEA to modulate potassium channels in Caco-2 cells, the FluxOR™ Potassium ion channel assay (ThermoFisher Scientific) was used. Briefly, Caco-2 cells were grown on 96 well plates until fully confluent and differentiated. Cells were loaded with the non-fluorescent, thallium specific FluxOR™ dye and then treated apically with increasing concentrations of OEA or PEA. When potassium channels are stimulated, thallium flows into the cell and binds the FluxOR™ dye, generating a fluorescent signal, proportional to channel activity, which was compared to the effects of a high potassium solution (Figure 1G).

Measurement of endocannabinoid levels

A quantitative LC-MS/MS method was used for analysis of OEA and PEA in cell samples, based on a previously reported procedure (51). For these experiments, Caco-2 cells were grown in T75 flasks and subjected to inflammatory conditions (10 $ng.ml^{-1}$ IFNγ for 8 h and 10 $ng.ml^{-1}$ TNFα for a further 16 h). Cell lysates and medium were stored at -80°C before analysis. Internal standard (0.42 nmol AEA-d8) was added to a 0.4 ml aliquot of each sample followed by solvent extraction (ethyl acetate: hexane; 9:1 v/v), centrifugation and evaporation. Prior to analysis, each sample extract was reconstituted in acetonitrile. An Applied Biosystems MDS SCIEX 4000 Q-Trap hybrid triple-quadrupole–linear ion trap mass spectrometer (Applied Biosystems, Foster City, CA, USA) operated in positive electrospray ionisation mode was used in conjunction with a Shimadzu series 10AD VP LC system (Shimadzu, Columbia, MD, USA) using an ACE 3 C8, 100 x 2.1 mm, 3 µm particle size column (Advanced Chromatography Technologies Ltd., Aberdeen, UK). Quantification was performed by measuring specific OEA and PEA precursor and product ions together with a calibrated internal standard method.

Chemicals and reagents

All chemicals and reagents used in these experiments were purchased from Sigma-Aldrich (Poole, UK) unless otherwise stated. OEA and PEA and the receptor antagonists AM251, AM630, GW9662, GW6471, capsazepine and O-1918 were purchased from Tocris (R&D Systems, UK). OEA and PEA were dissolved in ethanol to 10mM with further dilutions made in MEME. All receptors antagonists were dissolved in dimethyl sulfoxide (DMSO) to 10mM with further dilutions in MEME. Interferon-γ (IFNγ, 100μg) and Tumour Necrosis Factor-α (TNFα, 50μg) purchased from Invitrogen (Paisley, UK) and dilutions were made in fetal bovine serum (FBS).

Statistical analysis

Values are expressed as mean ± SEM. Time-course data was compared by 2 way, repeated measures (repeated by time factor) analysis of variance (ANOVA) using GraphPad Prism 6 (GraphPad Software, Inc., La Jolla, CA, USA). Statistical significance between manipulations and vehicle controls were determined by Dunnett's *post-hoc* test. $P<0.05$ was considered statistically significant.

Results

Permeability studies

Our initial experiments sought to explore whether the N-acylethanolamines were able to modulate the ionic conductance of the paracellular pathway, as a proxy for tight junction integrity. When applied to the apical membrane compartment, OEA increased Caco-2 cell monolayer transepithelial electrical resistance (TEER) (i.e. decreased permeability) in a concentration-dependent manner significantly different from control at 1, 3 and 10μM (Figure 1A). When applied to the basolateral membrane, OEA decreased TEER (i.e. increased permeability) in a concentration-dependent manner at 1, 3 and 10μM (Figure 1C). The Log EC_{50} of OEA at the apical membrane was -5.43 and at the basolateral membrane was -5.92 (see Supplemental Figure 1A).

PEA caused a large increase in TEER when applied to the apical membrane at 1, 3 and 10μM (Figure 1B). Although transient, the effects of 10 μM PEA remained significantly

above the effect of vehicle until 48 h post administration. When applied to the basolateral membrane, PEA increased resistance from 30 min post application in a concentration-dependent manner from 1 μM (Figure 1D). From 8 h post application, a significant effect of 300 nM PEA was observed. The Log EC_{50} of OEA at the apical membrane was -5.43 and at the basolateral membrane was -5.92 (see Supplemental Figure 1B,C).

To ensure that these changes in permeability were not related to changes in cell number, we carried out cell viability assays. Neither OEA nor PEA affected Caco-2 cell viability in fully confluent (see Supplemental Figure 2A) or proliferating (see Supplemental Figure 2B) cells. In addition, the expression of two aquaporins found in mammalian intestines (AQP3 and AQP4) that transport water, glycerol, ammonia and hydrogen peroxide (Kitchen 2015) and could impact on membrane permeability, was investigated. Apical treatment of Caco-2 cells with either OEA or PEA (10 μM, 1 h) led to a significant reduction in the membrane expression of AQP3 (Figure 1E) and AQP4 (Figure 1F). Furthermore, changes in transmembrane ion gradients generate osmotic alterations that can affect cell volume and the involvement of potassium ion influx in cell volume regulation has only recently been recognised (Pasantes-Morales 2016). Interestingly, apical treatment of Caco-2 cells with either OEA or PEA led to a concentration-independent increase in fluorescence indicative of activation of potassium channels (Figure 1G).

Cytoskeletal changes

In order to clarify the impact of these lipid mediators on cytoskeletal changes, mature Caco-2 cells were treated and processed to visualise F-actin (Figure 2). At the apical focal plane, cell to cell adhesion is visible across all treatments with no gaps (top panels). OEA rendered the cortical F-actin to have an irregular morphology (top, middle) compared to vehicle control (top left), whereas PEA induced focal adhesion plaques at sites of cell to cell adhesion (top right). Interestingly, cell adhesion to the slide can be seen at the basal focal plane in resting cells (bottom left), with OEA inducing a loss of both cellular tension through reduced actin filaments and focal adhesions (bottom middle). On the other hand, PEA caused an increase in polymerised F-actin filaments and focal adhesion plaques (bottom right). These occur throughout the cytoplasm of the cell, as well as some cortical accumulation. Images in Figure 3 are representative fields of view from 4 separate experiments. Full Z-stacks projected into single images can be viewed in Supplementary Figure 3.

Intracellular signalling

Since the action of the contractile cytoskeleton enables the cellular changes required to adjust permeability in response to its environment, we investigated the signalling events known to be important for cytoskeletal modifications, namely focal adhesion kinase (FAK) and the p42/44 MAP kinases (52). OEA induced a transient increase in both FAK and Erk1/2 (Figure 2, left panel, top and third blot down), peaking at 5 min and returning to basal levels by 30 min (Figure 3B,C). PEA induced phosphorylation of Erk1/2 to significant higher levels than OEA (Fig 3A, right panel, third blot down), but FAK activation by PEA continued to increase up to 1 hour post application (Fig 3B,C, right panel, top blot).

We carried out further experiments using Luminex technology and commercially available panels for multiple pathways and the SRC pathway. As seen with western blotting (Figure 1A), OEA significantly increased phosphorylated ERK1/2 and also p70s6K, CREB and NF_KB, and significantly decreased phosphorylated p38 and JNK (Figure 3D). PEA significantly increased phosphorylated ERK1/2, p70s6K, and CREB, and significantly decreased phosphorylated p38 (Figure 3E). In this panel, significant differences between OEA and PEA were observed in the ERK1/2 and Akt response (see Supplemental Figure 4D,F). In the Src family panel of signalling proteins, OEA and PEA significantly reduced phosphoylated Src, Yes, Lck, Lyn, Fgr, and Blk (significance is not shown in Figure 3F and G for clarity, please refer to Supplemental Figure 5). OEA also significantly reduced phosphoylated Fyn and Hck. This was more pronounced at 10 min for OEA (Figure 3F) and at 2 min for PEA (Figure 3G).

Receptor mechanism of action

The ability of a submaximal concentration of OEA (3 μM, apical application) to increase TEER was inhibited by capsazepine (a TRPV1 antagonist) only (Figure 4A). The ability of OEA (3 μM, basolateral) to decrease TEER was inhibited by the TRPV1 antagonist capsazepine and the PPARα receptor antagonist GW6471 (Figure 4C). The effect of PEA at the apical membrane was inhibited by the PPARα antagonist GW6471 (Figure 4B). The effect of PEA at the basolateral membrane was inhibited by a PPARα antagonist (Figure 4D).

OEA and PEA are degraded by fatty acid amid hydrolase (FAAH). When OEA or PEA were applied in combination with the FAAH inhibitor URB597, their effects were amplified. OEA (3 μM, apically) caused further increases in TEER when co-applied with a

FAAH inhibitor (URB597, Figure 5A) to the apical membrane, and this was inhibited by TRPV1 antagonism (Figure 5A). OEA (3 μM) also caused further decrease in resistance when co-applied with URB597 to the basolateral membrane, via TRPV1 and PPARα (Figure 5C). PEA (3 μM) caused further increases in resistance when co-applied with URB597 (at either the apical or basolateral membrane) and this was inhibited by the PPARα antagonist GW6471 (Figure 5B,D).

Effects of OEA and PEA on cytokine-induced hyperpermeability

When applied to the apical membrane concurrently with cytokines, OEA (3μM) prevented the fall in TEER (Figure 6A). Apically, OEA also recovered the increased permeability when applied 24h after cytokines (Figure 5B). By contrast, application of OEA to the basolateral membrane (at either time 0 or 24h) caused further decreases in TEER than caused by cytokines alone, indicating further increased permeability (Figure 6A,B).

PEA (3μM) prevented the drop in TEER caused by cytokines when applied at the same time to the basolateral membrane, evident at early as 8 h into the cytokine exposure (IFNγ exposure only, Figure 6A). This effect of PEA at the basolateral membrane was still observed when PEA was applied 24h after exposure to cytokines (Figure 6B). However, PEA has no effect on cytokine-increased permeability when applied to the apical membrane at either time-point (Figure 6A,B).

To establish whether OEA and PEA are produced endogenously in cells in response to simulated inflammatory conditions, cellular and secreted levels of these compounds were measured by LC-MS/MS after the inflammation protocol used to assess permeability changes. Cellular levels of OEA ($P<0.001$, Figure 6C) and PEA ($P<0.01$, Figure 5E) were significantly increased by the inflammatory protocol. Significantly raised levels of OEA ($P<0.0001$, Figure 6D) and PEA ($P<0.001$, Figure 6F) were also detectable in the medium in response to simulated inflammation.

Mechanisms of action of OEA and PEA on cytokine-induced hyperpermeability

When applied to the apical membrane concurrently with cytokines, as before (Figure 6), OEA (3μM) prevented the fall in TEER, and this effect was inhibited by the TRPV1 antagonist capsazepine (Figure 7A). Apically, OEA also recovered the increased permeability when applied 24h after cytokines, also inhibited by capsazepine (Figure 7C). As before,

application of OEA to the basolateral membrane caused further decrease in TEER (when added at time 0 or 24 h), which inhibited by the PPARα antagonist GW6471 but not capsazepine (Figure 7A,C).

As before, PEA (at the basolateral membrane) prevented the drop in TEER caused by cytokines when applied with at the same time or 24 h later, which was inhibited by GW6471 (Figure 7B,D).

The effects of OEA and PEA on prolonged cytokine exposure

Lastly, we examined whether OEA and PEA can alter the permeability response to prolonged cytokine exposure. 48 h after application of cytokines, apical application of OEA was able to restore permeability to baseline (Figure 8A). However, after 72 h inflammation, this ability of OEA was lost (Figure 8C). At the basolateral membrane, PEA was able to restore permeability to baseline when applied 48 h after cytokine exposure (Figure 8B) and even after 72 h after cytokine exposure (Figure 8D), and this effect of PEA was inhibited by the PPARα antagonist GW6471 (Figure 8D).

Discussion

This study has shown the effects of the endocannabinoid-like compounds OEA and PEA on the function and permeability of intestinal epithelial cells in control conditions and in inflammation. Both compounds were able to reverse the hyperpermeability associated with inflammatory conditions through different mechanisms; OEA through TRPV1 on the apical membrane, and PEA at the basolateral membrane through PPARα. Increased cellular and secreted OEA and PEA levels were observed in response to inflammation, suggesting their local release plays a role in intestinal permeability. Inhibition of the degradation of these compounds augmented their responses, indicating their effects are via the compounds themselves and not by their metabolites. It also suggests that the beneficial effects of these compounds could be augmented by co-administration of inhibitors of their degradation.

OEA

OEA production in the gut is stimulated by food intake (38) or reduced by food deprivation (39). OEA suppresses food intake, induces satiety and decreases body weight gain (43) via PPARα activation (44). In intestinal epithelial cells, under control conditions, we found that apical administration of OEA increased Caco-2 monolayer resistance (i.e. decreased permeability) in a concentration-dependent manner via TRPV1. In contrast, OEA increased permeability when applied to the basolateral membrane by activation of TRPV1 and PPARα receptors. Although it is not known whether OEA stimulation by food intake would occur at the basolateral or apical membrane, based on the findings of the present study, alterations in permeability are likely to be associated.

Contractile filamentous actin networks regulate cellular shape change, which can be spatially and temporally modulated during physiological processes such as cell adhesion, where cytoskeletal mechanics facilitate cell spreading and stiffening in response to environmental cues. F-actin structures such as lamella and stress fibres can facilitate adhesion, whereas cortical F-actin influences shape. FAK is a non-receptor protein kinase that can modulate barrier function (52), and our data confirms that OEA transiently activates FAK. However, the F-actin changes that ensue are twofold. Apically, the cortical arrangement indicates shape change, whereas basally, the filamentous structure was reduced. Reduced adhesion at the base of the cells could explain why OEA has a differential effect on TEER depending on where it is acting. It is unclear how the change in apical morphology connects to a change in cell-cell junctional complexes such that the interactions are tighter,

but certainly reduced cellular adhesion to the extracellular matrix (or glass slide in this instance) could account for the OEA effect on permeability when applied basally. It is important to note that cells remain attached to each other with no gaps, implying that the changes in permeability are not related to pore formation or destruction of the epithelial monolayer (also indicated by the lack of effect of OEA on cell viability).

There are many molecular markers that are associated with barrier integrity and membrane permeability. Apical junctional complex structure can be dynamic and the precise location of some of the component parts can influence the final outcome. The contribution and mechanisms of aquaporins in regulation of membrane permeability in the gut is unclear. In our study the reduction in AQP4 membrane protein expression by OEA was unlikely to affect water transport since knockdown of AQP4 does not impact on the colonic osmotic water permeability coefficient (53, 54), but could be related to other functions, such as the intestinal inflammatory response (55). With regard to AQP3, apical expression in the ileum is reduced in early IBD (56), which may be to limit excessive water loss or alleviate oxidative stress. However, Zhang and colleagues (57) did show that intestinal barrier integrity was impaired by the knockdown of AQP3 by enhancement of paracellular permeability. OEA lead to a modest reduction in expression of AQP3 in our study that would be unlikely to impact on TEER through water transport. The role of these aquaporins in glycerol and lipid metabolism is beyond the scope of this study, although it is tempting to speculate that the accepted contribution of OEA in fat sensing and transport of dietary lipids (58) could be mediated through aquaporin expression.

We also showed that OEA activated potassium channels in Caco-2 cells, which has been previously observed for OEA in arteries (59, 60). Potassium channel activation in the intestine is associated with many aspects of colonic epithelial function including regulating electrogenic transport, regulating cell volume and cellular migration (61, 62), suggesting OEA modulates epithelial cell functions in the intestine at many levels, which requires further investigation.

Regulation of the intercellular junctional interactions that maintain barrier function is highly complex. However, FAK activity through phosphorylation has been well correlated with TEER and that Src-dependency may be crucial to this function, particularly in Caco-2 cells (52). In our study, OEA transiently increased the autophosphorylation of FAK, but interestingly reduced Src phosphorylation in the same timeframe. Reduced phosphorylation of Src and JNK have been shown to attenuate stretch-induced reorganisation of the actin

cytoskeleton (63) and increased Src is associated with tight junction disruption in the intestinal epithelium (64). The increase in p70S6K and CREB phosphorylation is likely to relate to downstream gene transcription and protein translation, which is similar to PEA. However, the increase in NF-κB activity, which is unique to OEA in this system, requires further investigation. NF-κB has pleiotropic roles in cell survival and the immune response. The precise role of NF-kB in TEER in this context is unclear, but may explain the basolateral reduction in TEER, reminiscent of TNFα-induced barrier disruption (65).

In our model of inflammation, IFNγ and TNFα applied to the basolateral membrane of confluent Caco-2 cells increased permeability, similar to that previously reported by our group (35). We found that application of OEA apically, concurrently with the cytokines, or even after 24 or 48 hours later, reversed the increased permeability via TRPV1. This is the first study to investigate the effects of OEA on intestinal permeability in vitro, but OEA has been found to decrease blood brain barrier permeability in ischemia in vivo and in vitro, similarly by PPARα activation (66). Pharmacological activation of TRPV1 may contribute to colonic inflammation (30), thus the anti-inflammatory actions of OEA through TRPV1, may be brought about by desensitisation of the TRPV1 receptor. We also showed that inflammation significantly increased OEA levels in Caco-2 cells, suggesting these observations of the pharmacological effects of OEA have a physiological relevance. Others have similarly shown that OEA is upregulated in response to inflammation (67) or by feeding (68), and this may be as a result of increased OEA synthesis or reduced degradation.

To summarise the effects of OEA, at the apical membrane OEA decreases permeability and inhibits increased permeability when applied before or after the induction of increased permeability associated with inflammation via TRPV1 activation, and inflammation increases cellular levels of OEA. By contrast, at the basolateral membrane, OEA causes increased permeability through both TRPV1 and PPARα. Activation of FAK, inactivation of Src, changes in F-actin, activation of K^+ channels and downregulation of aquaporins may underlie these cellular responses to OEA.

PEA

PEA is currently available as a nutraceutical food for medical purposes under the brand names Normast®, Pelvilen® and PeaPure®, and has been studied in humans, mostly within trials on pain management, and is well tolerated (69). Several preclinical animal studies have shown that *in vivo* treatment with PEA reduces intestinal injury and inflammation via PPARα

(47, 48), and also CB_2 and GPR55 (49). In support of this, we showed that PEA decreases Caco-2 cell permeability when applied to either the apical or basolateral membrane in a time- and a concentration-dependent fashion, also via activation of the PPARα receptor. Furthermore, basolateral application of PEA, as might occur with systemic administration, also reversed the hyperpermeability associated with inflammation via PPARα. Unlike with OEA, there was no negative (i.e. increased permeability) response to PEA application at either membrane. In inflammation, this beneficial effect of PEA was observed when PEA was added before the insult, or even after 24, 48 and 72 hours post induction of inflammation. This ability of PEA to prevent increased permeability at the intestine barrier, via PPARα, is likely to underpin some of the beneficial effects seen *in vivo*. The increase in cellular PEA levels in response to our inflammatory protocol is in keeping with the proposed protective effects of endogenously produced PEA in the gut (70-72).

Like OEA, PEA also induced FAK activity, but the timing was more extended and the F-actin lamella structure seen with PEA was pronounced. These differences imply different cellular outcomes. The effect of PEA on the filament formation appears more typical in that FAK phosphorylation resulted in F-actin polymerisation and the filaments formed with focal adhesion plaques both at the apical cell to cell contacts and the "basement membrane" (glass slide in our case). Meaning that, functionally, these increases in turn increase cellular tension and adhesion to each other as well as to the "matrix"/adhesive surface, resulting in increased TEER regardless of whether applied apically or basally. Like OEA, PEA also led to a modest but significant reduction in both AQP3 and AQP4 in the membrane fraction and activated potassium channels (see earlier paragraph). The role of FAK activity in terms of transient and prolonged phosphorylation could have an impact on the transient versus sustained cytoskeletal changes that we see in this study. However, the rather blunt tool of immunoblotting may distort the rather more subtle contribution of location and binding partners.

To summarise the effects of PEA, at both the apical and basolateral membrane, PEA decreases permeability and inhibits increased permeability when applied before or up to 72 h after the induction of inflammation via PPARα, and inflammation increases cellular levels of PEA. Activation of FAK, inactivation of Src, changes in F-actin, activation of K^+ channels and downregulation of aquaporins may underlie these cellular responses. PEA treatment is feasible and tolerated in humans and the present studies provide a potential rationale to justify controlled clinical trials of PEA in gastrointestinal disorders.

Conclusion

OEA and PEA modulate intestinal permeability in normal and inflammatory conditions; OEA can both increase and decrease permeability (via TRPV1) when applied to the apical or basolateral membrane respectively, while PEA always decreases permeability i.e. increases resistance (via PPARα). Cellular levels of OEA and PEA are increased in intestinal epithelial cells in response to inflammation, which may limit the increased permeability associated with inflammation. The beneficial effects on intestinal permeability may at least partly underlie the protective effects of PEA on intestinal damage recently observed in preclinical studies. PPARα agonism, PEA administration or inhibiting PEA enzymatic degradation represent a novel range of therapeutic approaches against several intestinal disorders associated with increased intestinal permeability, including inflammatory bowel disease and acute intestinal ischaemia associated with circulatory shock.

Acknowledgements

We would like to thank Mrs Averil Warren and Mr Andy Lee for their technical assistance.

References

1. Helander, H. F., and Fandriks, L. (2014) Surface area of the digestive tract - revisited. *Scandinavian journal of gastroenterology* **49**, 681-689
2. Groschwitz, K. R., and Hogan, S. P. (2009) Intestinal barrier function: molecular regulation and disease pathogenesis. *The Journal of allergy and clinical immunology* **124**, 3-20; quiz 21-22
3. Ulluwishewa, D., Anderson, R. C., McNabb, W. C., Moughan, P. J., Wells, J. M., and Roy, N. C. (2011) Regulation of tight junction permeability by intestinal bacteria and dietary components. *The Journal of nutrition* **141**, 769-776
4. Turner, J. R. (2006) Molecular basis of epithelial barrier regulation: from basic mechanisms to clinical application. *The American journal of pathology* **169**, 1901-1909
5. Turner, J. R. (2009) Intestinal mucosal barrier function in health and disease. *Nature reviews. Immunology* **9**, 799-809
6. Brandtzaeg, P. (2011) The gut as communicator between environment and host: immunological consequences. *European journal of pharmacology* **668 Suppl 1**, S16-32
7. Welcker, K., Martin, A., Kolle, P., Siebeck, M., and Gross, M. (2004) Increased intestinal permeability in patients with inflammatory bowel disease. *European journal of medical research* **9**, 456-460
8. Sartor, R. B. (2006) Mechanisms of disease: pathogenesis of Crohn's disease and ulcerative colitis. *Nature clinical practice. Gastroenterology & hepatology* **3**, 390-407
9. Mankertz, J., and Schulzke, J. D. (2007) Altered permeability in inflammatory bowel disease: pathophysiology and clinical implications. *Current opinion in gastroenterology* **23**, 379-383

10. Hering, N. A., Fromm, M., and Schulzke, J. D. (2012) Determinants of colonic barrier function in inflammatory bowel disease and potential therapeutics. *The Journal of physiology* **590**, 1035-1044
11. Heyman, M., Abed, J., Lebreton, C., and Cerf-Bensussan, N. (2012) Intestinal permeability in coeliac disease: insight into mechanisms and relevance to pathogenesis. *Gut* **61**, 1355-1364
12. Dunlop, S. P., Hebden, J., Campbell, E., Naesdal, J., Olbe, L., Perkins, A. C., and Spiller, R. C. (2006) Abnormal intestinal permeability in subgroups of diarrhea-predominant irritable bowel syndromes. *The American journal of gastroenterology* **101**, 1288-1294
13. Camilleri, M., Lasch, K., and Zhou, W. (2012) Irritable bowel syndrome: methods, mechanisms, and pathophysiology. The confluence of increased permeability, inflammation, and pain in irritable bowel syndrome. *American journal of physiology. Gastrointestinal and liver physiology* **303**, G775-785
14. Camilleri, M., Madsen, K., Spiller, R., Greenwood-Van Meerveld, B., and Verne, G. N. (2012) Intestinal barrier function in health and gastrointestinal disease. *Neurogastroenterology and motility : the official journal of the European Gastrointestinal Motility Society* **24**, 503-512
15. Bischoff, S. C. (2011) 'Gut health': a new objective in medicine? *BMC medicine* **9**, 24
16. Hollander, D., Vadheim, C. M., Brettholz, E., Petersen, G. M., Delahunty, T., and Rotter, J. I. (1986) Increased intestinal permeability in patients with Crohn's disease and their relatives. A possible etiologic factor. *Annals of internal medicine* **105**, 883-885
17. May, G. R., Sutherland, L. R., and Meddings, J. B. (1993) Is small intestinal permeability really increased in relatives of patients with Crohn's disease? *Gastroenterology* **104**, 1627-1632
18. Wyatt, J., Oberhuber, G., Pongratz, S., Puspok, A., Moser, G., Novacek, G., Lochs, H., and Vogelsang, H. (1997) Increased gastric and intestinal permeability in patients with Crohn's disease. *The American journal of gastroenterology* **92**, 1891-1896
19. Odenwald, M. A., and Turner, J. R. (2013) Intestinal permeability defects: is it time to treat? *Clinical gastroenterology and hepatology : the official clinical practice journal of the American Gastroenterological Association* **11**, 1075-1083
20. Mechoulam, R. (1986) *The pharmacohistory of Cannabis sativa*, CRC Press
21. Mechoulam, R., Ben-Shabat, S., Hanus, L., Ligumsky, M., Kaminski, N. E., Schatz, A. R., Gopher, A., Almog, S., Martin, B. R., Compton, D. R., and et al. (1995) Identification of an endogenous 2-monoglyceride, present in canine gut, that binds to cannabinoid receptors. *Biochemical pharmacology* **50**, 83-90
22. Van Sickle, M. D., Oland, L. D., Ho, W., Hillard, C. J., Mackie, K., Davison, J. S., and Sharkey, K. A. (2001) Cannabinoids inhibit emesis through CB1 receptors in the brainstem of the ferret. *Gastroenterology* **121**, 767-774
23. Izzo, A. A., Fezza, F., Capasso, R., Bisogno, T., Pinto, L., Iuvone, T., Esposito, G., Mascolo, N., Di Marzo, V., and Capasso, F. (2001) Cannabinoid CB1-receptor mediated regulation of gastrointestinal motility in mice in a model of intestinal inflammation. *British journal of pharmacology* **134**, 563-570
24. Adami, M., Frati, P., Bertini, S., Kulkarni-Narla, A., Brown, D. R., de Caro, G., Coruzzi, G., and Soldani, G. (2002) Gastric antisecretory role and immunohistochemical localization of cannabinoid receptors in the rat stomach. *British journal of pharmacology* **135**, 1598-1606
25. Maccarrone, M., and Finazzi-Agro, A. (2003) The endocannabinoid system, anandamide and the regulation of mammalian cell apoptosis. *Cell death and differentiation* **10**, 946-955
26. Klein, T. W. (2005) Cannabinoid-based drugs as anti-inflammatory therapeutics. *Nature reviews. Immunology* **5**, 400-411

27. Di Marzo, V., and Izzo, A. A. (2006) Endocannabinoid overactivity and intestinal inflammation. *Gut* **55**, 1373-1376
28. Di Carlo, G., and Izzo, A. A. (2003) Cannabinoids for gastrointestinal diseases: potential therapeutic applications. *Expert opinion on investigational drugs* **12**, 39-49
29. Pertwee, R. G. (1997) Pharmacology of cannabinoid CB1 and CB2 receptors. *Pharmacology & therapeutics* **74**, 129-180
30. Massa, F., Sibaev, A., Marsicano, G., Blaudzun, H., Storr, M., and Lutz, B. (2006) Vanilloid receptor (TRPV1)-deficient mice show increased susceptibility to dinitrobenzene sulfonic acid induced colitis. *J Mol Med-Jmm* **84**, 142-146
31. O'Sullivan, S. E. (2007) Cannabinoids go nuclear: evidence for activation of peroxisome proliferator-activated receptors. *British journal of pharmacology* **152**, 576-582
32. Fredriksson, R., Hoglund, P. J., Gloriam, D. E., Lagerstrom, M. C., and Schioth, H. B. (2003) Seven evolutionarily conserved human rhodopsin G protein-coupled receptors lacking close relatives. *FEBS letters* **554**, 381-388
33. Ryberg, E., Larsson, N., Sjogren, S., Hjorth, S., Hermansson, N. O., Leonova, J., Elebring, T., Nilsson, K., Drmota, T., and Greasley, P. J. (2007) The orphan receptor GPR55 is a novel cannabinoid receptor. *British journal of pharmacology* **152**, 1092-1101
34. Alhamoruni, A., Lee, A. C., Wright, K. L., Larvin, M., and O'Sullivan, S. E. (2010) Pharmacological Effects of Cannabinoids on the Caco-2 Cell Culture Model of Intestinal Permeability. *Journal of Pharmacology and Experimental Therapeutics* **335**, 92-102
35. Alhamoruni, A., Wright, K. L., Larvin, M., and O'Sullivan, S. E. (2012) Cannabinoids mediate opposing effects on inflammation-induced intestinal permeability. *British journal of pharmacology* **165**, 2598-2610
36. Muccioli, G. G., Naslain, D., Backhed, F., Reigstad, C. S., Lambert, D. M., Delzenne, N. M., and Cani, P. D. (2010) The endocannabinoid system links gut microbiota to adipogenesis. *Molecular systems biology* **6**, 392
37. Piomelli, D., Beltramo, M., Giuffrida, A., and Stella, N. (1998) Endogenous cannabinoid signaling. *Neurobiology of disease* **5**, 462-473
38. Astarita, G., Rourke, B. C., Andersen, J. B., Fu, J., Kim, J. H., Bennett, A. F., Hicks, J. W., and Piomelli, D. (2006) Postprandial increase of oleoylethanolamide mobilization in small intestine of the Burmese python (Python molurus). *Am J Physiol-Reg I* **290**, R1407-R1412
39. Izzo, A. A., Piscitelli, F., Capasso, R., Marini, P., Cristino, L., Petrosino, S., and Di Marzo, V. (2010) Basal and fasting/refeeding-regulated tissue levels of endogenous PPAR-alpha ligands in Zucker rats. *Obesity (Silver Spring, Md.)* **18**, 55-62
40. Fu, J., Gaetani, S., Oveisi, F., Lo Verme, J., Serrano, A., de Fonseca, F. R., Rosengarth, A., Luecke, H., Di Giacomo, B., Tarzia, G., and Piomelli, D. (2003) Oleylethanolamide regulates feeding and body weight through activation of the nuclear receptor PPAR-alpha. *Nature* **425**, 90-93
41. Ahern, G. P. (2003) Activation of TRPV1 by the satiety factor oleoylethanolamide. *The Journal of biological chemistry* **278**, 30429-30434
42. Borrelli, F., and Izzo, A. A. (2009) Role of acylethanolamides in the gastrointestinal tract with special reference to food intake and energy balance. *Best practice & research. Clinical endocrinology & metabolism* **23**, 33-49
43. Rodriguez de Fonseca, F., Navarro, M., Gomez, R., Escuredo, L., Nava, F., Fu, J., Murillo-Rodriguez, E., Giuffrida, A., LoVerme, J., Gaetani, S., Kathuria, S., Gall, C., and Piomelli, D. (2001) An anorexic lipid mediator regulated by feeding. *Nature* **414**, 209-212
44. Lo Verme, J., Gaetani, S., Fu, J., Oveisi, F., Burton, K., and Piomelli, D. (2005) Regulation of food intake by oleoylethanolamide. *Cellular and Molecular Life Sciences* **62**, 708-716

45. Guzman, M., Lo Verme, J., Fu, J., Oveisi, F., Blazquez, C., and Piomelli, D. (2004) Oleoylethanolamide stimulates lipolysis by activating the nuclear receptor peroxisome proliferator-activated receptor alpha (PPAR-alpha). *Journal of Biological Chemistry* **279**, 27849-27854
46. Fu, J., Oveisi, F., Gaetani, S., Lin, E., and Piomelli, D. (2005) Oleoylethanolamide, an endogenous PPAR-alpha agonist, lowers body weight and hyperlipidemia in obese rats. *Neuropharmacology* **48**, 1147-1153
47. Esposito, G., Capoccia, E., Turco, F., Palumbo, I., Lu, J., Steardo, A., Cuomo, R., Sarnelli, G., and Steardo, L. (2014) Palmitoylethanolamide improves colon inflammation through an enteric glia/toll like receptor 4-dependent PPAR-alpha activation. *Gut* **63**, 1300-1312
48. Di Paola, R., Impellizzeri, D., Torre, A., Mazzon, E., Cappellani, A., Faggio, C., Esposito, E., Trischitta, F., and Cuzzocrea, S. (2012) Effects of palmitoylethanolamide on intestinal injury and inflammation caused by ischemia-reperfusion in mice. *J Leukoc Biol* **91**, 911-920
49. Borrelli, F., Romano, B., Petrosino, S., Pagano, E., Capasso, R., Coppola, D., Battista, G., Orlando, P., Di Marzo, V., and Izzo, A. A. (2015) Palmitoylethanolamide, a naturally-occurring lipid, is an orally effective intestinal anti-inflammatory agent. *British journal of pharmacology* **doi: 10.1111/bph.12907**
50. Alhouayek, M., Lambert, D. M., Delzenne, N. M., Cani, P. D., and Muccioli, G. G. (2011) Increasing endogenous 2-arachidonoylglycerol levels counteracts colitis and related systemic inflammation. *Faseb Journal* **25**, 2711-2721
51. Richardson, D., Ortori, C. A., Chapman, V., Kendall, D. A., and Barrett, D. A. (2007) Quantitative profiling of endocannabinoids and related compounds in rat brain using liquid chromatography-tandem electrospray ionization mass spectrometry. *Analytical biochemistry* **360**, 216-226
52. Ma, Y., Semba, S., Khan, R. I., Bochimoto, H., Watanabe, T., Fujiya, M., Kohgo, Y., Liu, Y., and Taniguchi, T. (2013) Focal adhesion kinase regulates intestinal epithelial barrier function via redistribution of tight junction. *Biochimica et biophysica acta* **1832**, 151-159
53. Ma, T., Yang, B., Gillespie, A., Carlson, E. J., Epstein, C. J., and Verkman, A. S. (1997) Generation and phenotype of a transgenic knockout mouse lacking the mercurial-insensitive water channel aquaporin-4. *The Journal of clinical investigation* **100**, 957-962
54. Wang, K. S., Ma, T., Filiz, F., Verkman, A. S., and Bastidas, J. A. (2000) Colon water transport in transgenic mice lacking aquaporin-4 water channels. *American journal of physiology. Gastrointestinal and liver physiology* **279**, G463-470
55. Hansen, J. J., Holt, L., and Sartor, R. B. (2009) Gene expression patterns in experimental colitis in IL-10-deficient mice. *Inflammatory bowel diseases* **15**, 890-899
56. Ricanek, P., Lunde, L. K., Frye, S. A., Stoen, M., Nygard, S., Morth, J. P., Rydning, A., Vatn, M. H., Amiry-Moghaddam, M., and Tonjum, T. (2015) Reduced expression of aquaporins in human intestinal mucosa in early stage inflammatory bowel disease. *Clinical and experimental gastroenterology* **8**, 49-67
57. Zhang, W., Xu, Y., Chen, Z., Xu, Z., and Xu, H. (2011) Knockdown of aquaporin 3 is involved in intestinal barrier integrity impairment. *FEBS letters* **585**, 3113-3119
58. Piomelli, D. (2013) A fatty gut feeling. *Trends in endocrinology and metabolism: TEM* **24**, 332-341
59. Wheal, A. J., Alexander, S. P., and Randall, M. D. (2010) Vasorelaxation to N-oleoylethanolamine in rat isolated arteries: mechanisms of action and modulation via cyclooxygenase activity. *British journal of pharmacology* **160**, 701-711
60. AlSuleimani, Y. M., and Hiley, C. R. (2013) Mechanisms of vasorelaxation induced by oleoylethanolamide in the rat small mesenteric artery. *European journal of pharmacology* **702**, 1-11

61. Rao, J. N., Platoshyn, O., Li, L., Guo, X., Golovina, V. A., Yuan, J. X., and Wang, J. Y. (2002) Activation of K(+) channels and increased migration of differentiated intestinal epithelial cells after wounding. *American journal of physiology. Cell physiology* **282**, C885-898
62. Heitzmann, D., and Warth, R. (2008) Physiology and pathophysiology of potassium channels in gastrointestinal epithelia. *Physiological reviews* **88**, 1119-1182
63. Samak, G., Gangwar, R., Crosby, L. M., Desai, L. P., Wilhelm, K., Waters, C. M., and Rao, R. (2014) Cyclic stretch disrupts apical junctional complexes in Caco-2 cell monolayers by a JNK-2-, c-Src-, and MLCK-dependent mechanism. *American journal of physiology. Gastrointestinal and liver physiology* **306**, G947-958
64. Basuroy, S., Sheth, P., Kuppuswamy, D., Balasubramanian, S., Ray, R. M., and Rao, R. K. (2003) Expression of kinase-inactive c-Src delays oxidative stress-induced disassembly and accelerates calcium-mediated reassembly of tight junctions in the Caco-2 cell monolayer. *The Journal of biological chemistry* **278**, 11916-11924
65. Ma, T. Y., Iwamoto, G. K., Hoa, N. T., Akotia, V., Pedram, A., Boivin, M. A., and Said, H. M. (2004) TNF-alpha-induced increase in intestinal epithelial tight junction permeability requires NF-kappa B activation. *American journal of physiology. Gastrointestinal and liver physiology* **286**, G367-376
66. Zhou, Y., Yang, L., Ma, A., Zhang, X., Li, W., Yang, W., Chen, C., and Jin, X. (2012) Orally administered oleoylethanolamide protects mice from focal cerebral ischemic injury by activating peroxisome proliferator-activated receptor alpha. *Neuropharmacology* **63**, 242-249
67. Pontis, S., Ribeiro, A., Sasso, O., and Piomelli, D. (2016) Macrophage-derived lipid agonists of PPAR-alpha as intrinsic controllers of inflammation. *Critical reviews in biochemistry and molecular biology* **51**, 7-14
68. Fu, J., Astarita, G., Gaetani, S., Kim, J., Cravatt, B. F., Mackie, K., and Piomelli, D. (2007) Food intake regulates oleoylethanolamide formation and degradation in the proximal small intestine. *The Journal of biological chemistry* **282**, 1518-1528
69. Schifilliti, C., Cucinotta, L., Fedele, V., Ingegnosi, C., Savoca, G., and Leotta, C. (2011) Palmitoylethanolamide Reduces the Symptoms of Neuropathic Pain in Diabetic Patients. *Shock* **36**, 30-30
70. Borrelli, F., Romano, B., Petrosino, S., Pagano, E., Capasso, R., Coppola, D., Battista, G., Orlando, P., Di Marzo, V., and Izzo, A. A. (2015) Palmitoylethanolamide, a naturally occurring lipid, is an orally effective intestinal anti-inflammatory agent. *British journal of pharmacology* **172**, 142-158
71. Wang, J., Zheng, J., Kulkarni, A., Wang, W., Garg, S., Prather, P. L., and Hauer-Jensen, M. (2014) Palmitoylethanolamide regulates development of intestinal radiation injury in a mast cell-dependent manner. *Dig Dis Sci* **59**, 2693-2703
72. Capasso, R., Orlando, P., Pagano, E., Aveta, T., Buono, L., Borrelli, F., Di Marzo, V., and Izzo, A. A. (2014) Palmitoylethanolamide normalizes intestinal motility in a model of post-inflammatory accelerated transit: involvement of CB(1) receptors and TRPV1 channels. *British journal of pharmacology* **171**, 4026-4037

Figure 1. *The effects of OEA and PEA on Caco-2 cell permeability and function*. Concentration-response curves to OEA applied either apically (A) or basolaterally (C) and to PEA applied apically (B) and basolaterally (D) on Caco-2 cell monolayers permeability (n=3). Data are given as means and standard error bars S.E.M., * P<0.05, ** P< 0.01, *** P<0.001, comparing between control and experimental data by 2 way repeated measures ANOVA. E. The effects of OEA and PEA (both 10 μM, 1 h treatment) on the expression of aquaporin 3 (E) and aquaporin 4 (F) in the membrane fraction of Caco2 cells. G. The effect of OEA and PEA on and on potassium channel activation. Data are given as means and standard error bars S.E.M., * P<0.05, *** P<0.001, comparing between control and experimental data by 1 way ANOVA.

Figure 2. *F-actin cytoskeletal networks in mature Caco-2 cells.* Cells were grown to confluence and fully differentiated on glass chamberslides. Fresh complete medium was applied before the addition of compounds for 1h. Cells were then fixed and stained with phalloidin and DAPI, as per methods and images were captured using confocal microscope. *Left panels*, vehicle control (VC, ethanol); *middle panels*, OEA (10mM) and *right panels*, PEA (10mM). From a total of 26 Z-stacks, the *top panels* are representative images of an apical focal plane and, *bottom panels,* of basal focal planes taken as close to the adhesion surface (glass slide) as possible. Images are representative fields of view from 4 separate experiments. Full Z-stacks projected into single images can be viewed in *supplementary data*. Scale bar = 10mm.

Figure 3. *The effects of OEA and PEA on signalling proteins*. A. A representative blot of the effects of OEA and PEA on focal adhesion kinase (FAK) and the p42/44 MAP kinases and the mean densitometric analysis of A (B and C, n=4). Luminex® xMAP® technology was used to detect changes in phosphorylated CREB (pS133), ERK (pT185/pY187), NFkB (pS536), JNK (pT183/pY185), p38 (pT180/pY182), p70 S6K (pT412), STAT3 (pS727), STAT5A/B (pY694/699) and Akt (pS473) (Milliplex™, 48-680MAG, Merck Millipore) in cell lysates for OEA (D) and PEA (E). Luminex® xMAP® technology was also used to detect changes in phosphorylated Blk (Tyr389), Fgr (Tyr412), Fyn (Tyr420), Hck (Tyr411), Lck (Tyr394), Lyn (Tyr397), Src (Tyr419) and Yes (Tyr421)(Milliplex™, 48-650MAG Human Src Family kinase, Merck Millipore) in cell lysates for OEA (D) and PEA (E). Data was analysed by 2-way ANOVA. Data are given as means with error bars representing S.E.M. Data was analysed by 2-way ANOVA. * denotes a significant difference compared to control.

Figure 4. Receptor mechanism of action for OEA and PEA modulation of Caco-2 permeability. The effects of OEA applied to the apical (A) or basolateral (B) side of the Caco-2 monolayer alone and in combination with various receptor antagonists. The effects of PEA applied to the apical side (C) or basolateral (D) side of the Caco-2 monolayer alone and in combination with various receptor antagonists. Data are given as means with error bars representing SEM (n=3-6).

Figure 5. The effects of fatty acid amide hydrolase (FAAH) inhibition on OEA and PEA modulation of Caco-2 permeability. The effects of OEA applied to the apical (A) or basolateral (C) side of the Caco-2 monolayer alone and in the presence of the FAAH inhibitor (URB597, 1μM) in combination with receptor antagonists. The effects of PEA applied to the apical side (B) or basolateral (D) side of the Caco2 monolayer

alone and in the presence of URB597 in combination with receptor antagonists. Data are given as means with error bars representing SEM (n = 3).

Figure 6. The effects of OEA and PEA in a model of increased permeability induced by cytokines. The effect of OEA and PEA (3μM) on the permeability induced by cytokines (10ng/ml) when applied apically and basolaterally at 0h (A), or 24h after the induction of inflammation (B). Data are given as means with error bars representing SEM (n = 3, *P<0.01, **P<0.01, ***P<0.001, 2 way repeated measures ANOVA with post hoc analysis comparing against the vehicle control data). The solid bar represents the time of cytokine exposure and arrow denotes application of OEA/PEA. C-F. Cells were grown to confluence in T75 flasks (n=6 per condition) and exposed to the inflammation protocol. OEA and PEA levels were measured by mass spectrometry in the cellular lysate (C,E) or medium (D,F). Data is presented as mean ± SEM and were analysed by Student t-test. *** P<0.001, ****P<0.0001.

Figure 7. The target sites of action for OEA and PEA in a model of increased permeability induced by cytokines. The effect of OEA and PEA (3μM) in the presence of various receptor antagonists on the permeability induced by cytokines when applied apically and basolaterally at 0h (A,B), or 24h after the induction of inflammation (C,D). Data are given as means with error bars representing SEM (n = 3, *P<0.01, **P<0.01, ***P<0.001, 2 way repeated measures ANOVA with post hoc Dunnett's test comparing against the vehicle control data.

Figure 8. PEA rescues permeability after prolonged cytokine exposure. The effects of OEA and PEA on cytokine induced increased permeability when applied after 48h inflammation (A, B) or after 72 h inflammation (C,D). Data are given as means with error bars representing SEM (n=3-6, ***P< 0.001, ****P<0.0001), and was analysed by 2 way ANOVA with Dunnett's post hoc test comparing against the vehicle control data.

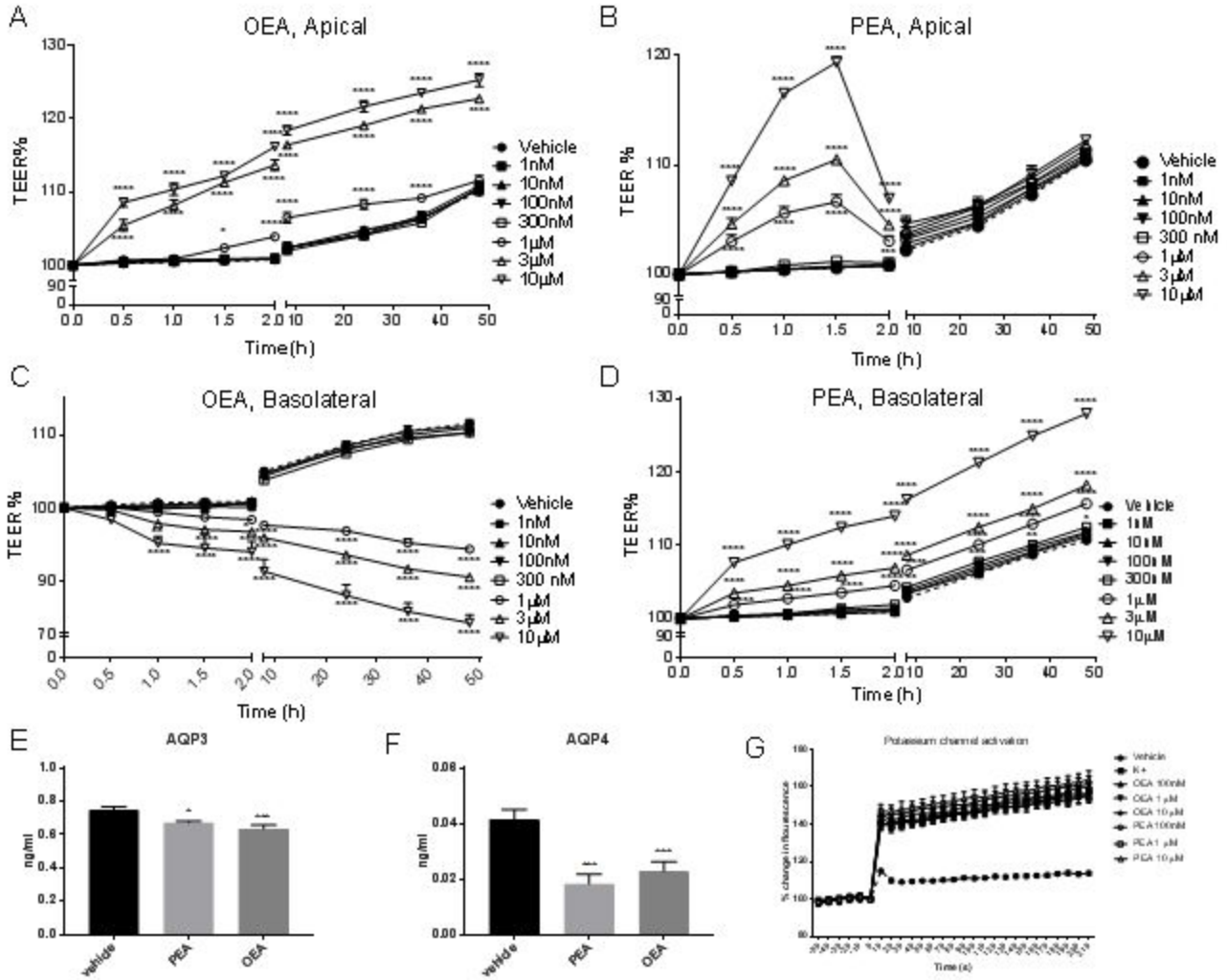

Figure 1. *The effects of OEA and PEA on Caco-2 cell permeability and function.* Concentration-response curves to OEA applied either apically (A) or basolaterally (C) and to PEA applied apically (B) and basolaterally (D) on Caco-2 cell monolayers permeability (n=3). Data are given as means and standard error bars S.E.M., * P<0.05, ** P< 0.01, *** P<0.001, comparing between control and experimental data by 2 way repeated measures ANOVA. E. The effects of OEA and PEA (both 10 µM, 1 h treatment) on the expression of aquaporin 3 (E) and aquaporin 4 (F) in the membrane fraction of Caco2 cells. G. The effect of OEA and PEA on potassium channel activation. Data are given as means and standard error bars S.E.M., * P<0.05, *** P<0.001, comparing between control and experimental data by 1 way ANOVA.

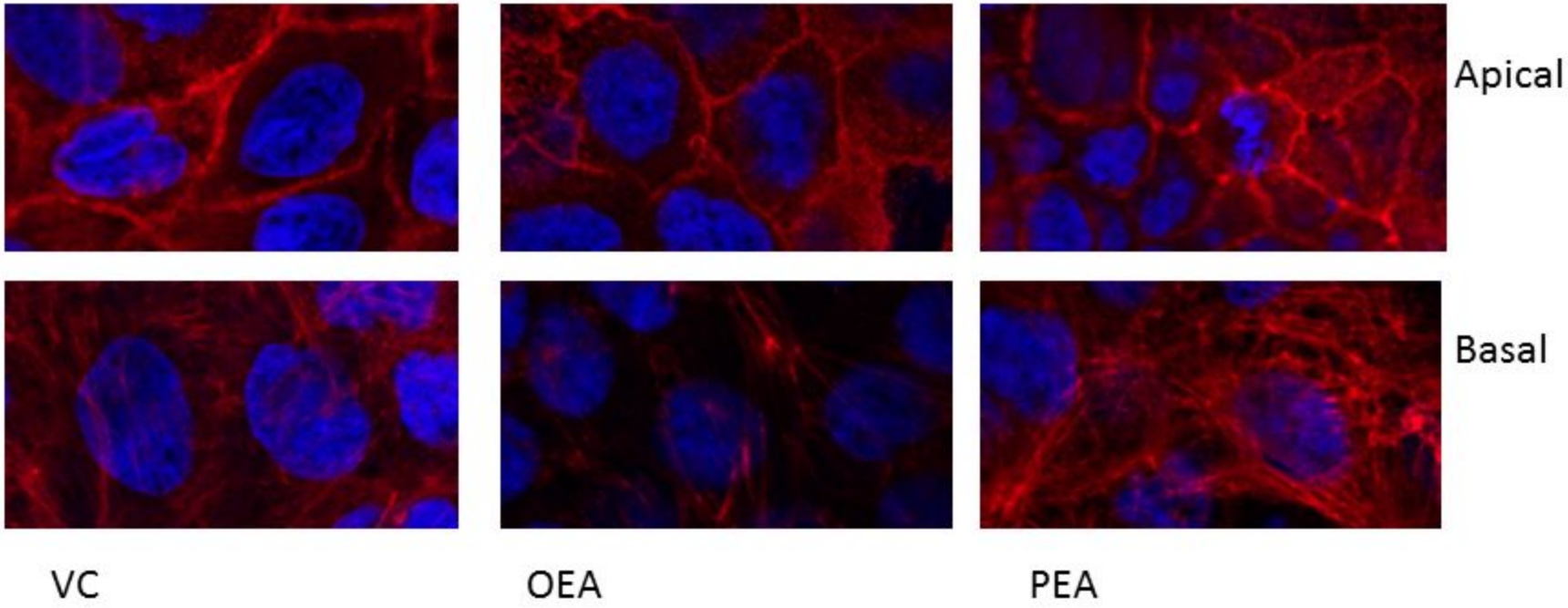

Figure 2. *F-actin cytoskeletal networks in mature Caco-2 cells.* Cells were grown to confluence and fully differentiated on glass chamberslides. Fresh complete medium was applied before the addition of compounds for 1h. Cells were then fixed and stained with phalloidin and DAPI, as per methods and images were captured using confocal microscope. *Left panels*, vehicle control (VC, ethanol); *middle panels*, OEA (10µM) and *right panels*, PEA (10µM). From a total of 26 Z-stacks, the *top panels* are representative images of an apical focal plane and, *bottom panels,* of basal focal planes taken as close to the adhesion surface (glass slide) as possible. Images are representative fields of view from 4 separate experiments. Full Z-stacks projected into single images can be viewed in *supplementary data*. Scale bar = 10µm.

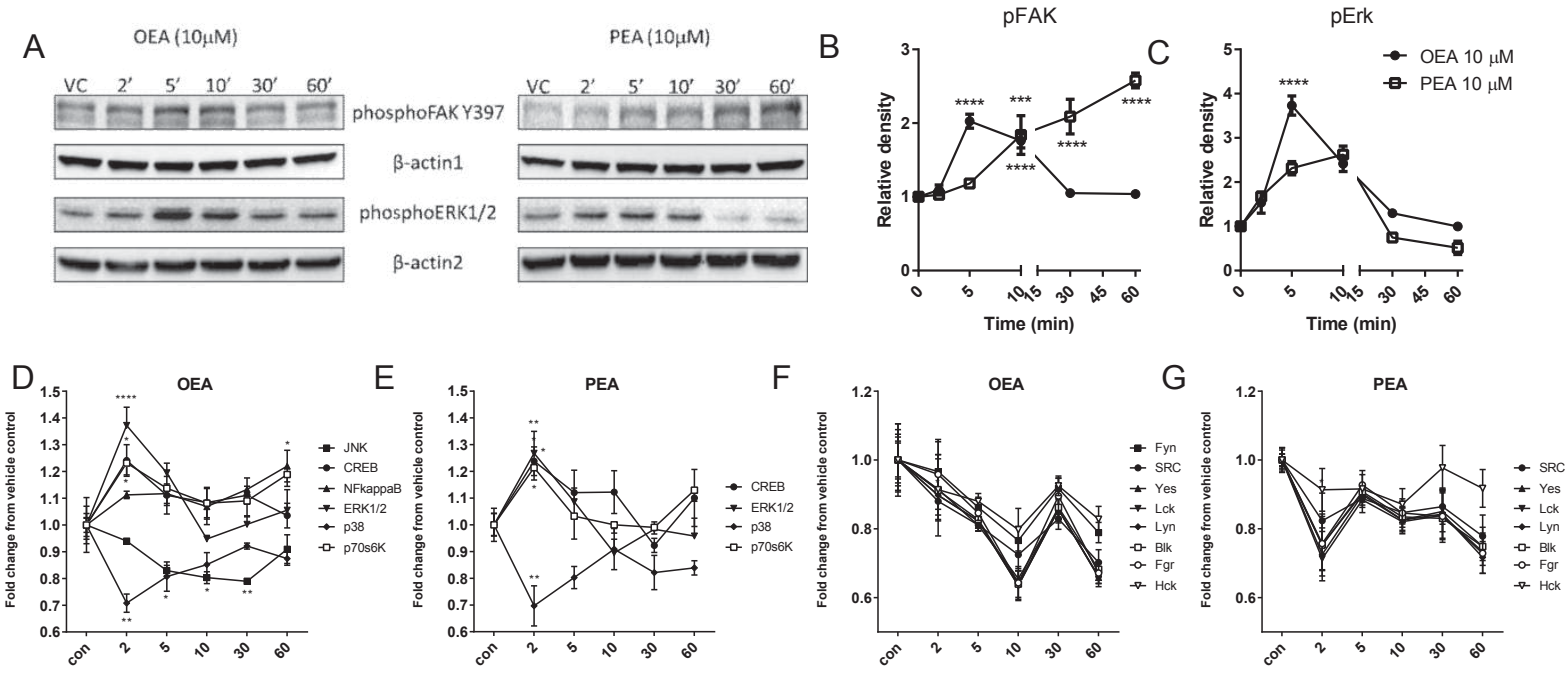

Figure 3. *The effects of OEA and PEA on signalling proteins*. A. A representative blot of the effects of OEA and PEA on focal adhesion kinase (FAK) and the p42/44 MAP kinases and the mean densitometric analysis of A (B and C, n=4). Luminex® xMAP® technology was used to detect changes in phosphorylated CREB (pS133), ERK (pT185/pY187), NFkB (pS536), JNK (pT183/pY185), p38 (pT180/pY182), p70 S6K (pT412), STAT3 (pS727), STAT5A/B (pY694/699) and Akt (pS473) (Milliplex™, 48-680MAG, Merck Millipore) in cell lysates for OEA (D) and PEA (E). Luminex® xMAP® technology was also used to detect changes in phosphorylated Blk (Tyr389), Fgr (Tyr412), Fyn (Tyr420), Hck (Tyr411), Lck (Tyr394), Lyn (Tyr397), Src (Tyr419) and Yes (Tyr421)(Milliplex™, 48-650MAG Human Src Family kinase, Merck Millipore) in cell lysates for OEA (D) and PEA (E). Data was analysed by 2-way ANOVA. Data are given as means with error bars representing S.E.M. Data was analysed by 2-way ANOVA. * denotes a significant difference compared to control

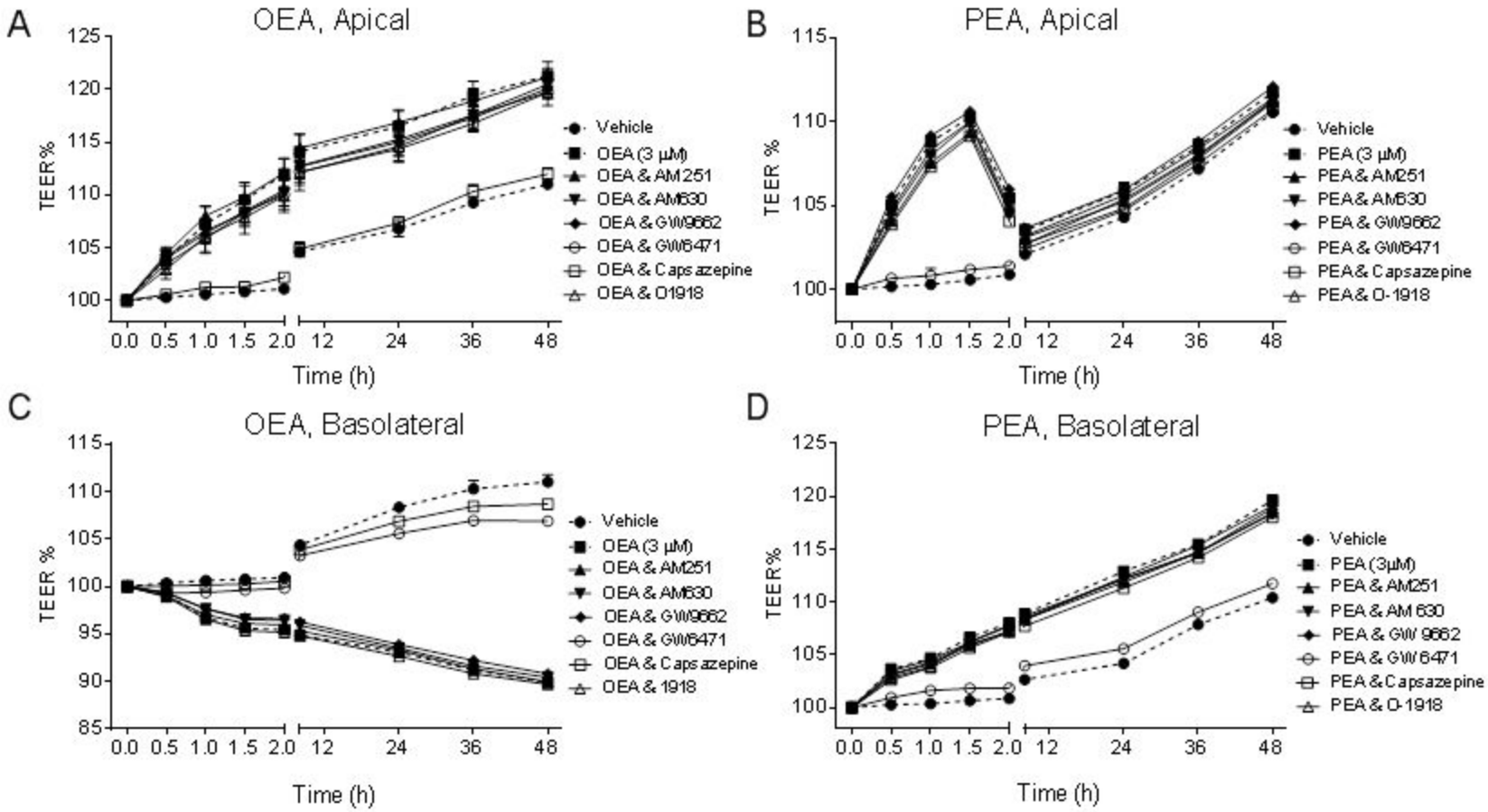

Figure 4. *Receptor mechanism of action for OEA and PEA modu lation of Caco-2 permeability.* The effects of OEA applied to the apical (A) or basolateral (B) side of the Caco-2 monolayer alone and in combination with various receptor antagonists. The effects of PEA applied to the apical side (C) or basolateral (D) side of the Caco-2 monolayer alone and in combination with various receptor antagonists. Data are given as means wi th error bars representing SEM (n=3-6).

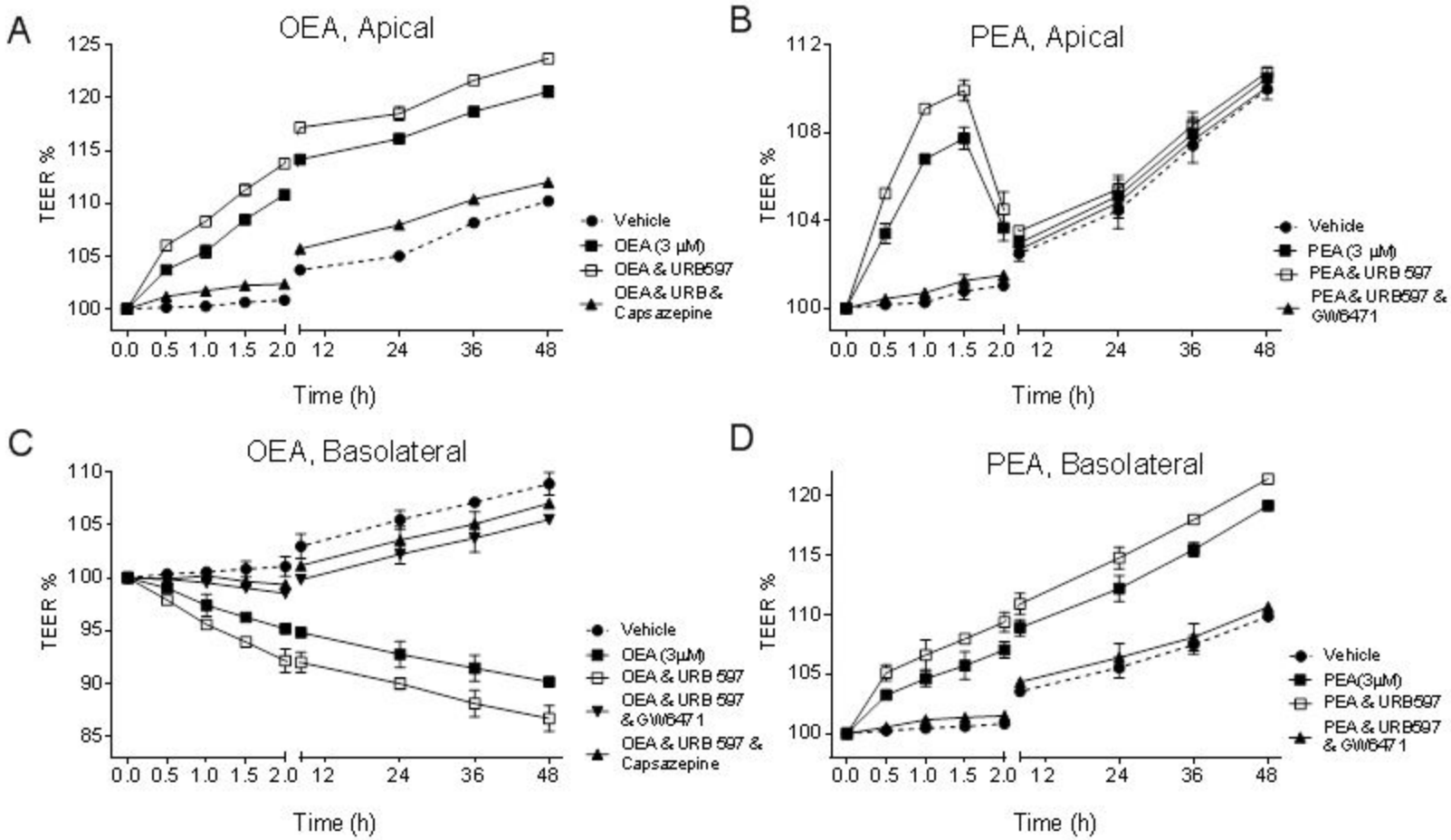

Figure 5. *The effects of fatty acid amide hydrolase (FAAH) inhibition on OEA and PEA modulation of Caco-2 permeability*. The effects of OEA applied to the apical (A) or basolateral (C) side of the Caco-2 monolayer alone and in the presence of the FAAH inhibitor (URB597, 1µM) in combination with receptor antagonists . The effects of PEA applied to the apical side (B) or basolateral (D) side of the Caco2 monolayer alone and in the presence of URB597 in combination with receptor antagonists. Data are given as means with error bars representing SEM (n = 3).

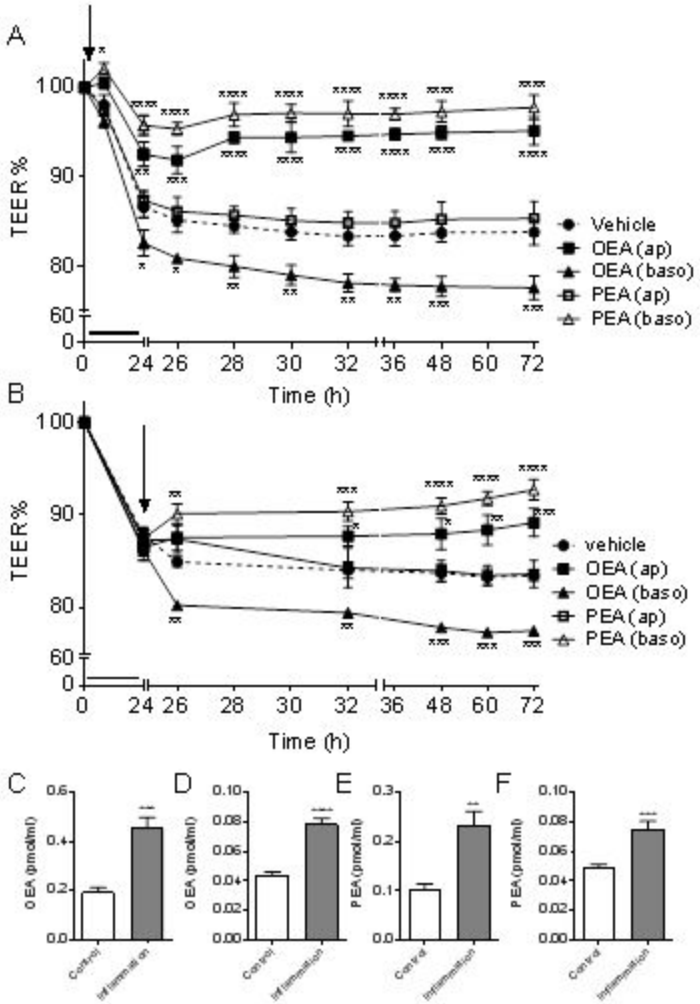

Figure 6. *The effects of OEA and PEA in a model of increased permeability induced by cytokines.* The effect of OEA and PEA (3μM) on the permeability induced by cytokines (10ng/ml) when applied apically and basolaterally at 0h (A), or 24h after the induction of inflammation (B). Data are given as means with error bars representing SEM (n = 3, *P<0.01, **P<0.01, ***P< 0.001, 2 way repeated measures ANOVA with post hoc analysis comparing against the vehicle control data). The solid bar represents the time of cytokine exposure and arrow denotes application of OEA/PEA. C-F. Cells were grown to confluence in T75 flasks (n=6 per condition) and exposed to the inflammation protocol. OEA and PEA levels were measured by mass spectrometry in the cellular lysate (C,E) or medium (D,F). Data is presented as mean ± SEM and were analysed by Student t-test. *** P<0.001, ****P<0.0001.

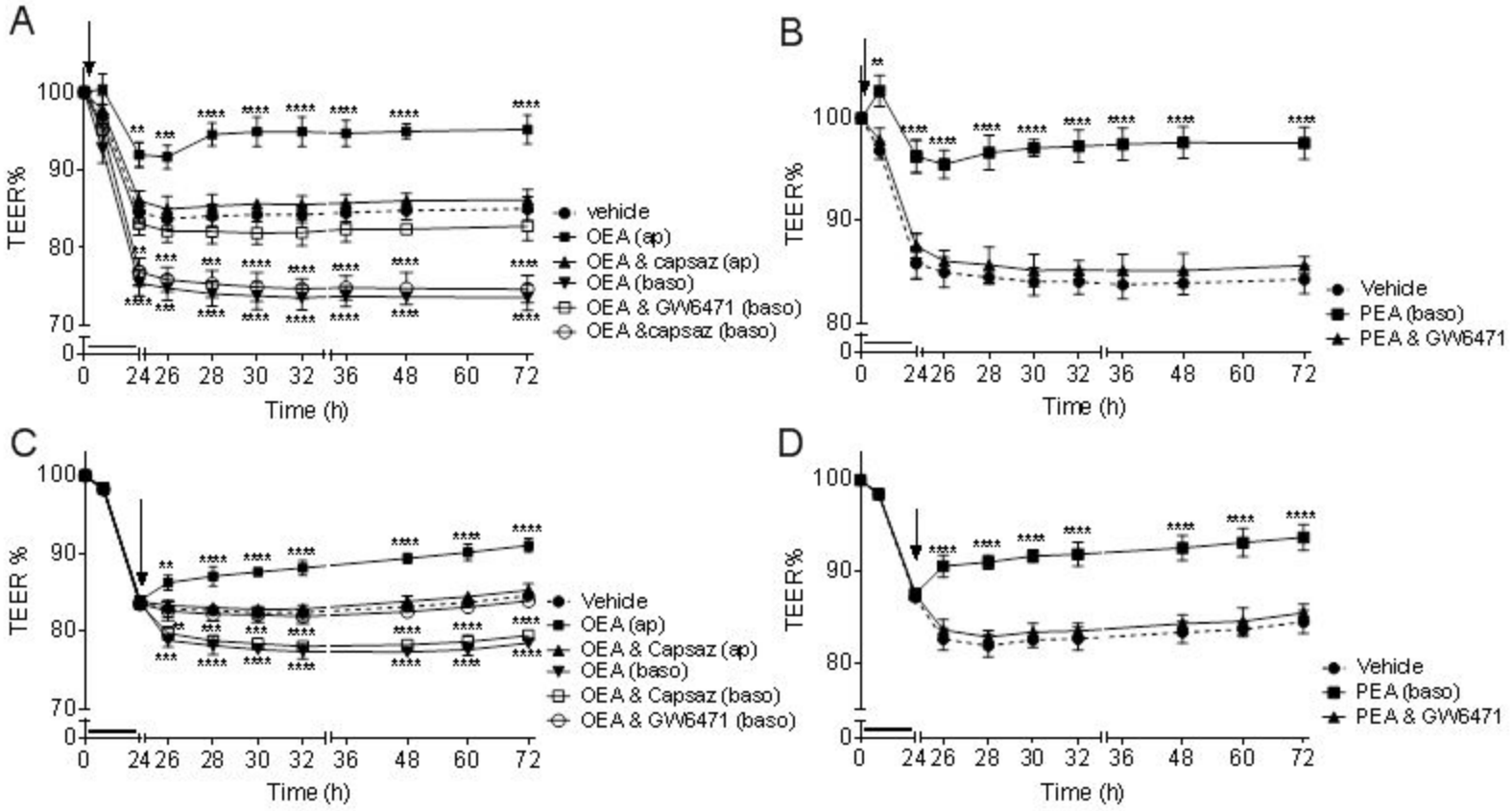

Figure 7. *The target sites of action for OEA and PEA in a model of increased permeability induced by cytokines.* The effect of OEA and PEA (3μM) in the presence of various receptor antagonists on the permeability induced by cytokines when applied apically and basolaterally at 0h (A,B), or 24h after the induction of inflammation (C,D). Data are given as means w ith error bars representing SEM (n = 3, *P<0.01, **P<0.01, ***P< 0.001, 2 way repeated measures ANOVA with post hoc Dunnett's test comparing against the vehicle control data .

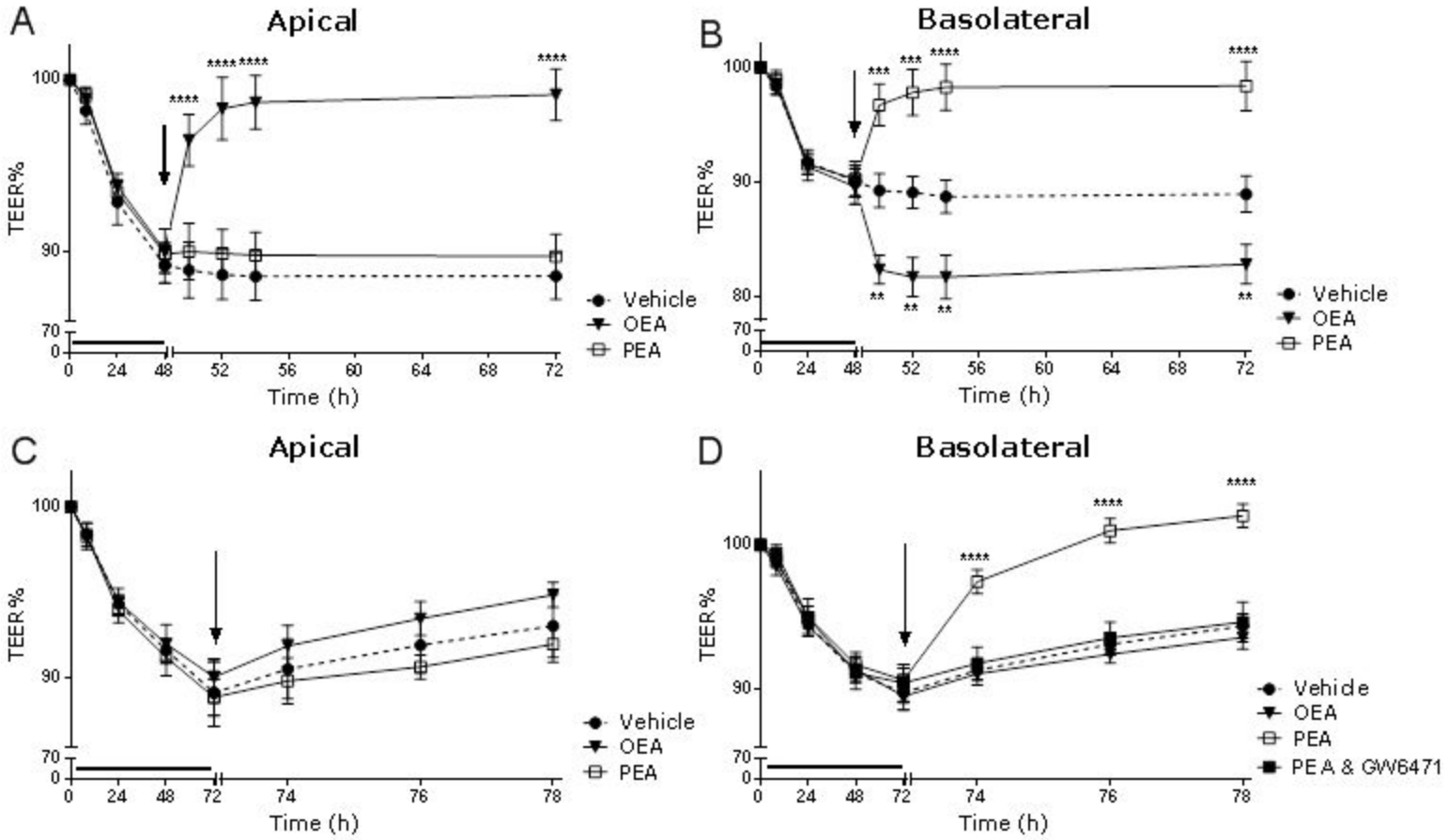

Figure 8. *PEA rescues permeability after prolonged cytokine exposure.* The effects of OEA and PEA on cytokine induced increased permeability when applied after 48h inflammation (A, B) or after 72 h inflammation (C,D). Data are given as means with error bars representing SEM (n=3-6, ***P< 0.001, ****P<0.0001), and was analysed by 2 way ANOVA with Dunnett's post hoc test comparing against the vehicle control data .

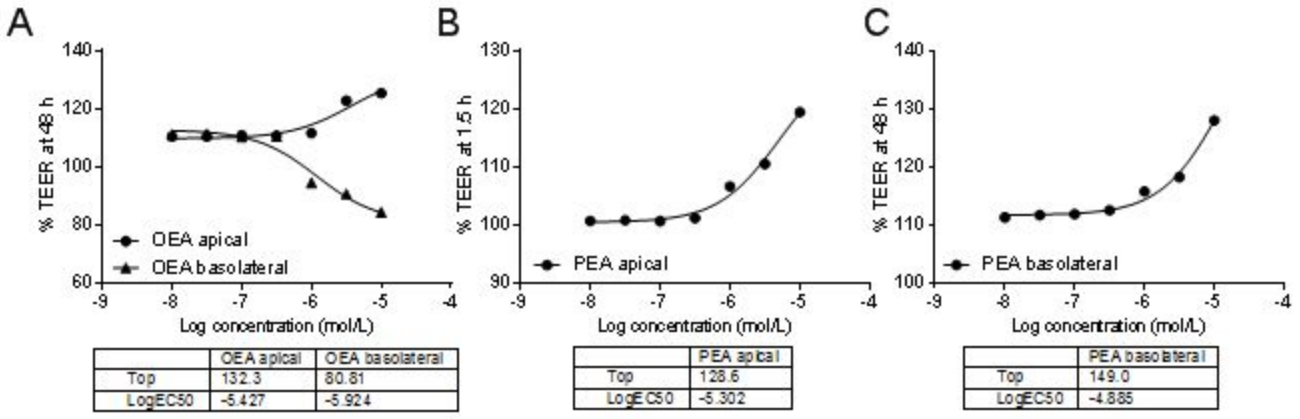

	OEA apical	OEA basolateral
Top	132.3	80.81
LogEC50	-5.427	-5.924

	PEA apical
Top	128.6
LogEC50	-5.302

	PEA basolateral
Top	149.0
LogEC50	-4.885

Supplemental Figure 1. Concentration response curves of the effects of OEA and PEA at the apical (A,B) and basolateral (A,C) membrane on Caco-2 permeability. For A and C, the maximal effects of OEA or PEA were taken at the 48h timepoint from Figure 1. For B, the maximal effect of PEA at the apical membrane was taken at the 1.5h timepoint from Figure 1.

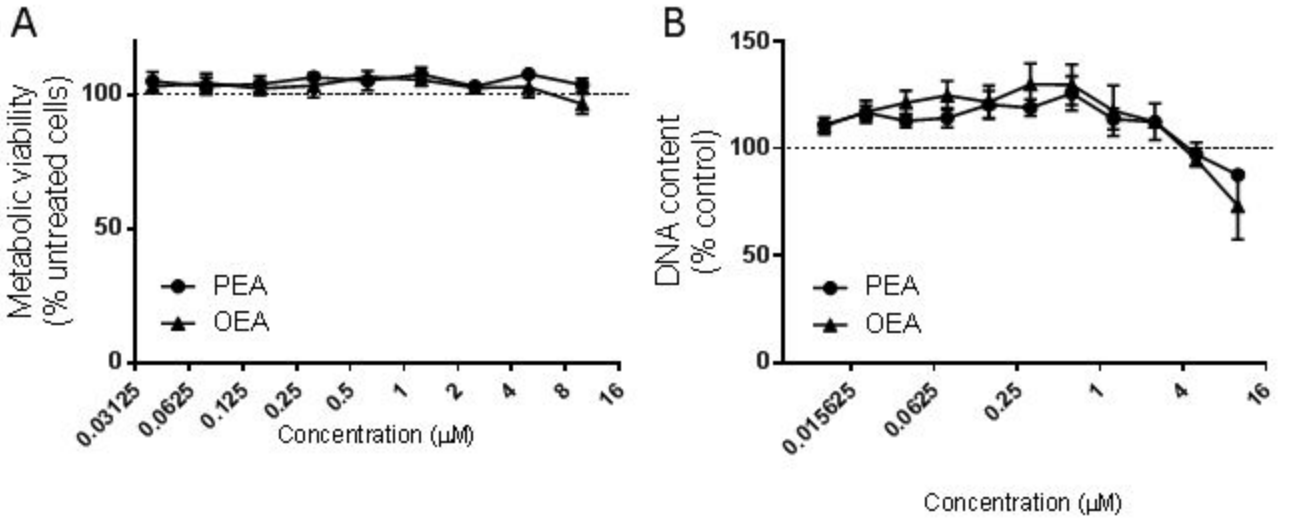

Supplemental Figure 2. A. The effects of OEA and PEA (48 h treatment) on Caco-2 cell viability in fully confluent and differentiated cells (n=4) using PrestoBlue™ Reagent. B. The effects of OEA and PEA (72 h treatment) on Caco-2 cell viability in proliferating cells (B, n=3) using CyQUANT®NF dye reagent. Data are given as means with error bars representing S.E.M.

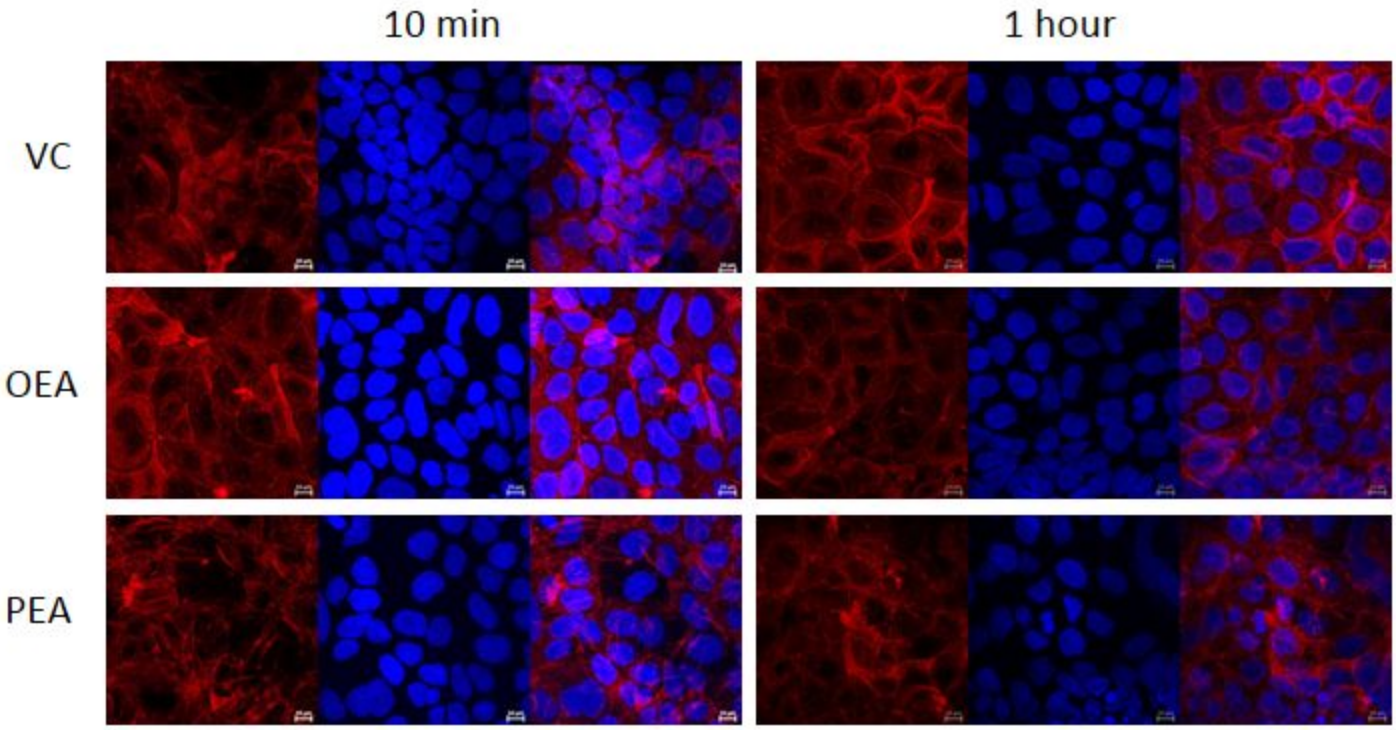

Supplementary Figure 3. *F-actin cytoskeletal networks in mature Caco-2 cells.* Cells were grown to confluence and fully differentiated on glass chamberslides. Fresh complete medium was applied before the addition of compounds for the times indicated. Cells were then fixed and stained with phalloidin, as per methods and images were captured using confocal microscope. *Top panel*, vehicle control (VC, ethanol); *middle panel*, OEA (10mM) and *bottom panel*, PEA (10mM). Images are representative fields of view from 4 separate experiments with full Z-stacks projected into a single image. Scale bar = 10mm.

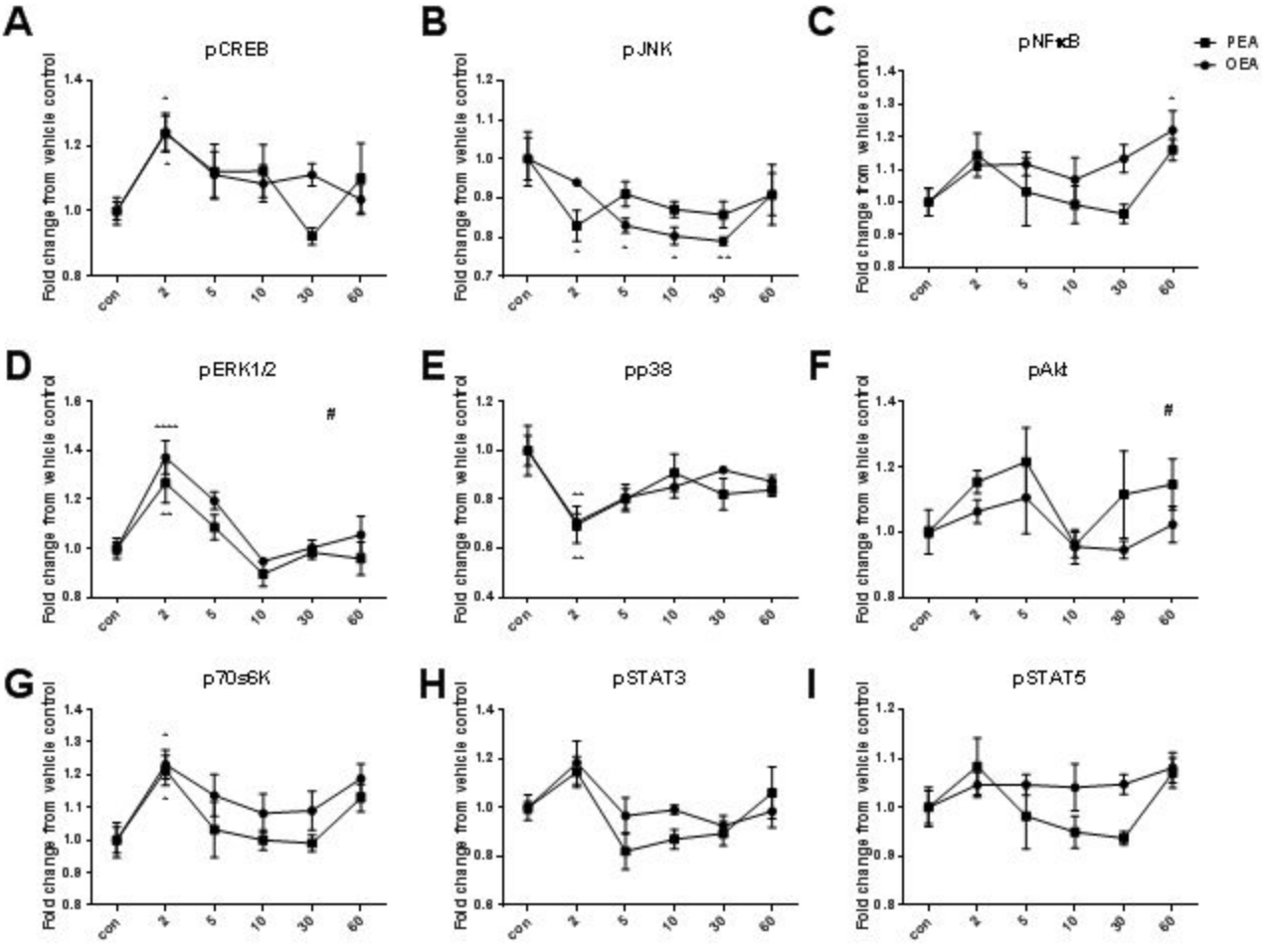

Supplemental Figure 4.The temporal effects of OEA and PEA (10 μM) on key signalling proteins. Luminex® xMAP® technology was used to detect changes in phosphorylated CREB (pS133), ERK (pT185/pY187), NFκB (pS536), JNK (pT183/pY185), p38 (pT180/pY182), p70 S6K (pT412), STAT3 (pS727), STAT5A/B (pY694/699) and Akt (pS473) (Milliplex™, 48-680MAG, Merck Millipore) in cell lysates. Data was analysed by 2-way ANOVA. * denotes a significant difference compared to control. # denotes a significant difference between OEA and PEA. (* or # P<0.05, **P<0.01, *** P<0.001, ****P<0.0001).

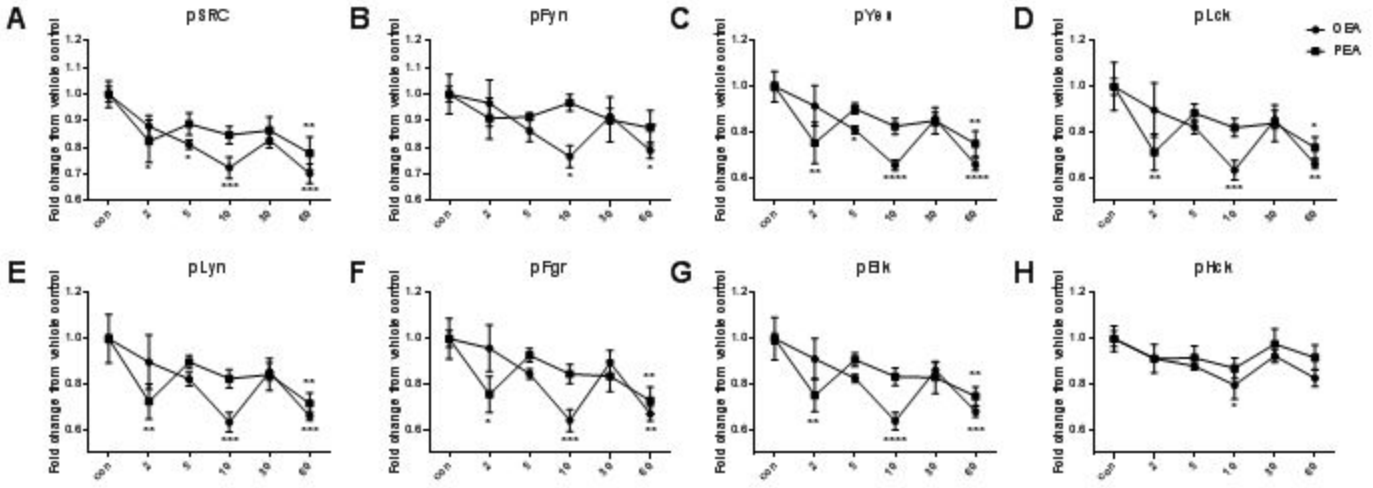

Supplemental Figure 5.The temporal effects of OEA and PEA (10 μM) on key signalling proteins. Luminex® xMAP® technology was used to detect changes in phosphorylated Blk (Tyr389), Fgr (Tyr412), Fyn (Tyr420), Hck (Tyr411), Lck (Tyr394), Lyn (Tyr397), Src (Tyr419) and Yes (Tyr421)(Milliplex™, 48-650MAG Human Src Family kinase, Merck Millipore) in cell lysates. Data was analysed by 2-way ANOVA. * denotes a significant difference compared to control. (* P<0.05, **P<0.01, *** P<0.001, ****P<0.0001).